THE EFFECT OF REUSED POWDER CHARACTERISTICS ON THE PROPERTIES OF ADDITIVELY MANUFACTURED 17-4 PH STAINLESS STEEL

A THESIS SUBMITTED TO
THE GRADUATE SCHOOL OF NATURAL AND APPLIED SCIENCES
OF
MIDDLE EAST TECHNICAL UNIVERSITY

BY

ECE KAHRAMAN

IN PARTIAL FULFILLMENT OF THE REQUIREMENTS
FOR
THE DEGREE OF MASTER OF SCIENCE
IN
METALLURGICAL AND MATERIALS ENGINEERING

APRIL 2022

Approval of the thesis:

THE EFFECT OF REUSED POWDER CHARACTERISTICS ON THE PROPERTIES OF ADDITIVELY MANUFACTURED 17-4 PH STAINLESS STEEL

submitted by **ECE KAHRAMAN** in partial fulfillment of the requirements for the degree of **Master of Science** i**n Metallurgical and Materials Engineering, Middle East Technical University** by,

Prof. Dr. Halil Kalıpçılar
Dean, Graduate School of **Natural and Applied Sciences** _____

Prof. Dr. C. Hakan Gür
Head of the Department, **Metallurgical and Materials Eng.** _____

Prof. Dr. Bilgehan Ögel
Supervisor, **Metallurgical and Materials Eng., METU** _____

Assist. Prof. Dr. Evren Yasa
Co-Supervisor, **Mechanical Eng., Eskişehir Osmangazi University** _____

Examining Committee Members:

Prof. Dr. Rıza Gürbüz
Metallurgical and Materials Eng, METU _____

Prof. Dr. Bilgehan Ögel
Metallurgical and Materials Eng, METU _____

Assist. Prof. Dr. Özgür Poyraz
Mechanical Engineering, Eskişehir Technical University _____

Prof. Dr. Ali Kalkanlı
Metallurgical and Materials Eng, METU _____

Prof. Dr. C. Hakan Gür
Metallurgical and Materials Eng, METU _____

Date: 25.04.2022

I hereby declare that all information in this document has been obtained and presented in accordance with academic rules and ethical conduct. I also declare that, as required by these rules and conduct, I have fully cited and referenced all material and results that are not original to this work.

Name Last name : Ece Kahraman

Signature :

ABSTRACT

THE EFFECT OF REUSED POWDER CHARACTERISTICS ON THE PROPERTIES OF ADDITIVELY MANUFACTURED 17-4 PH STAINLESS STEEL

Kahraman, Ece
Master of Science, Metallurgical and Materials Engineering
Supervisor: Prof. Dr. Bilgehan Ögel
Co-Supervisor: Assist. Prof. Dr. Evren Yasa

April 2022, 96 pages

Powder bed additive manufacturing methods use the powder form of the material of the part to be produced as raw material. The quality of the production is highly dependent on the properties of the powder used in the first place. Consistently using new unused powder for each new additive manufacturing is costly and removes the advantage of additive manufacturing, i.e. low amount of waste material. In powder bed additive manufacturing methods, powders are laid layer by layer and melted by laser or electron beam to form the final piece. Since the areas determined according to the CAD data of the part in each layer are scanned and melted, the surrounding powders remain unmelted and at the end of the production, the part is cleaned from the remaining powders. Bringing these remained powders back into another production is cost-effective. However, it is important not to compromise on the quality of the parts. Therefore, it is necessary to investigate the effects of reusing metal powders on additive manufacturing parts. In this thesis, the effects of powder reuse on the properties of selective laser melted 17-4 PH stainless steel were investigated. Using the same powder, 10 successive productions were carried out. In the productions, it is aimed to increase the thermal history of the powders as much as possible by producing geometries in a way that the powders will be most affected

by the laser. Samples were taken from the powders in accordance with the standards before the first production and after the last production. These samples were subjected to various tests such as shape analysis, dimensional analysis and chemical composition analysis. In addition, block parts and tensile test specimens were produced in order to examine the part properties in certain productions. As a result of reuse of the powders 10 times, no change was observed in the powder shapes, bulk densities, particle size distribution and mechanical properties of the obtained parts. However, the tapped density value of the reused powder increased by 7.7% compared to the unused powder. In addition, it was determined that the oxygen ratio increased by 16% and the nitrogen ratio increased by 17% in reused powders. It is evaluated that with the further increase of the reuse cycle of the powder, the powders will become more contaminated and the raw material will go out of specification.

Keywords: Additive Manufacturing, Powder Characterization, Metal Powder Reuse, Selective Laser Melting

ÖZ

TEKRARLI KULLANILAN TOZ ÖZELLİKLERİNİN EKLEMELİ İMALAT İLE ÜRETİLMİŞ 17-4 PH PASLANMAZ ÇELİK ÖZELLİKLERİ ÜZERİNDEKİ ETKİSİ

Kahraman, Ece
Yüksek Lisans, Metalurji ve Malzeme Mühendisliği
Tez Yöneticisi: Prof. Dr. Bilgehan Ögel
Ortak Tez Yöneticisi: Dr. Öğr. Üyesi Evren Yasa

Nisan 2022, 96 sayfa

Toz yataklı eklemeli imalat yöntemleri hammadde olarak üretilmek istenen parçanın malzemesinin toz formunu kullanır. Üretimin kalitesi en başta kullanılan tozun özelliklerine oldukça bağlıdır. Her bir yeni eklemeli imalat üretiminde sürekli olarak yeni, kullanılmamış, toz kullanmak maliyet açısından oldukça zorlayıcı olmaktadır. Oysa ki her bir eklemeli imalat prosesinde ekipmana beslenen tozların çoğu prosesten ana parçaya katılmadan toz formunda tekrar çıkmaktadır. Bu tozların tekrardan bir diğer üretime kazandırılması maliyet açısından yararlı bir durum olmaktadır. Ancak parça kalitesinde de ödün verilmemesi önemli bir husustur. Bu nedenle metal tozlarının tekrar kullanımın eklemeli imalat parçaları üzerindeki etkilerinin araştırılması gereği doğmaktadır. Bu tez çalışmasında toz yataklı eklemeli imalat yöntemlerinden bir tanesi olan seçici lazer ergitme metodu ile üretilen 17-4 PH paslanmaz çelik parçalarda tozun yeniden kullanımın etkileri yapılan deneyler ile desteklenerek incelenmiştir. Birbirini takip eden 10 üretim sadece aynı tozların tekrar tekrar kullanılması ile gerçekleştirilmiştir. Üretimlerde tozların lazerden en çok etkileneceği şekilde geometriler üretilerek tozların olabilecek en çok miktarda ısıl geçmişinin artırılması hedeflenmiştir. Tozlardan ilk üretim öncesi ve son üretim

sonrası standartlara uygun şekilde numuneler alınmıştır. Bu numuneler şekil analizi, boyut analizi ve kimyasal kompozisyon analizi gibi çeşitli testlere tabii tutulmuştur. Ayrıca belirli üretimlerde parça özelliklerinin incelenebilmesi açısından blok parçalar ve çekme kuponları üretilmiştir. Tozların 10 defa tekrar kullanımı sonucu toz şekillerinde, yığın yoğunluklarında, parçacık büyüklüğü dağılımında ve elde edilen parçaların mekanik özelliklerinde değişim gözlenmemiştir. Ancak, tekrar kullanılan tozun sıkıştırılmış yoğunluk değeri kullanılmamış toza göre %7.7 oranında artmıştır. Ayrıca tekrar kullanılan tozlarda oksijen oranının %16, nitrojen oranının %17 oranında arttığı saptanmıştır. Tozun tekrar kullanım döngüsünün daha da artırılması ile tozların daha fazla kontamine olacağı ve hammalzemenin spesifikasyon dışına çıkacağı değerlendirilmektedir.

Anahtar Kelimeler: Eklemeli İmalat, Toz Karakterizasyonu, Metal Tozu Yeniden Kullanımı, Seçici Lazer Ergitme

To my beloved family

ACKNOWLEDGMENTS

I would like to thank my advisor, Prof. Dr. Bilgehan Ögel, for always supporting my thesis work, guiding my way with precious ideas and for being a source of motivation for me in every situation.

I am grateful to my co-advisor Assist. Prof. Dr. Evren Yasa for making this thesis come true and for encouraging me to continue my research in all circumstances.

I would like to thank Prof. Dr. Ali Kalkanlı for making a great contribution to the realization of my thesis experiments and for taking the thesis to the next level with his valuable ideas.

I would like to express my deepest gratitude to my colleagues Andaç Özsoy, Mert Keleş, Erkan Buğra Türeyen, Hüseyin Ayaş and Ahmet Kösem who have always supported me during my thesis experiments. I would like to express my sincere thanks to Mertcan Başkan who paved the way for my improvement in powder characterization and the development of my thesis. My most special thanks go to Orkun Umur Önem who has been with me since the first steps of my thesis.

I also owe my warmest thank to my dear friends Beyza Kütük, Okay Tutar, Tansu Göynük, and Dilara Peker, who instilled faith in me during the realization of my thesis. I would also like to express my most valuable thanks to my dear friend Oğuzcan Dedeci who was always by my side and supported me during productions and tests in this thesis and with whom I had a storm of ideas while interpreting the results.

Finally, I would like to express my greatest gratitude to my dear family, who have always supported me throughout my thesis studies, provided motivation in all circumstances, brought me to where I am today, and made me always look to the future with hope. I would like to express my heartfelt thanks to my dear husband, my soulmate, Ufuk Ulaş. I am grateful to you for always supporting me during my thesis work and for always making me smile.

TABLE OF CONTENTS

LIST OF TABLES

TABLES

LIST OF FIGURES

FIGURES

CHAPTER 1

INTRODUCTION

Thanks to the high chromium content, stainless steels form a protective film layer on their surfaces, and the presence of this layer gives the steels the feature of being rustproof. Although there are many types of stainless steels, precipitation hardened stainless steels, which are frequently used in the aerospace industry, have become very popular. These stainless steels are subject to precipitation hardening due to the elements they contain such as copper and niobium. These stainless steel group, which generally serves up to 300°C without being damaged, can find a place for itself in many areas from the aviation industry to the medical fields. The most favorite material of the precipitation hardened stainless steels group is 17-4 precipitation hardening (PH) stainless steel. As the name suggests, this steel contains 17% chromium and 4% nickel. It is a martensitic stainless steel. With the precipitation of the copper element in its content, it has an advantageous hardness in many applications. They are also known for having good corrosion resistance and strength. Additive manufacturing method in the production of 17-4 PH stainless steel stands out as an eye-catching method in the industry world. With this method, the product is created layer by layer so that very complex geometries that cannot be obtained with conventional methods can be produced [1]. Although there are seven groups of additive manufacturing methods according to ASTM F2792-12a (2013) Standard Terminology for Additive Manufacturing Technologies [2], the most commonly utilized with the highest maturity level is the powder-bed fusion group. Under powder-bed fusion group, electron beam melting and selective laser melting (SLM) method are the mostly used processes for metallic materials. Due to advantages of very highly complex geometries with internal features and fine details as well as high

surface quality, SLM, also known as laser beam powder bed fusion (LB-PBF) is more preferred in comparison to EBM (also known as electron beam powder bed fusion EB-PBF). In the SLM process, metal powder particles are laid layer by layer and melted by laser, and products are produced in the desired shape. The properties of the built parts directly depend on the powder characteristics making the raw material inspection very critical. Powders must be of absolute quality so that the final product is a quality and defect-free part that can meet the requirements. Although for some materials, there are powder standards defining the powder characteristics for AM such as F2924-14 (2021) Standard Specification for Additive Manufacturing Titanium-6 Aluminum-4 Vanadium with Powder Bed Fusion [3] and F3055-14a (2021) Standard Specification for Additive Manufacturing Nickel Alloy (UNS N07718) with Powder Bed Fusion [4], these guidelines are generally not satisfactory defining in the absolute limits of material properties and insufficient in terms of defining key performance indicators for powder reuse.

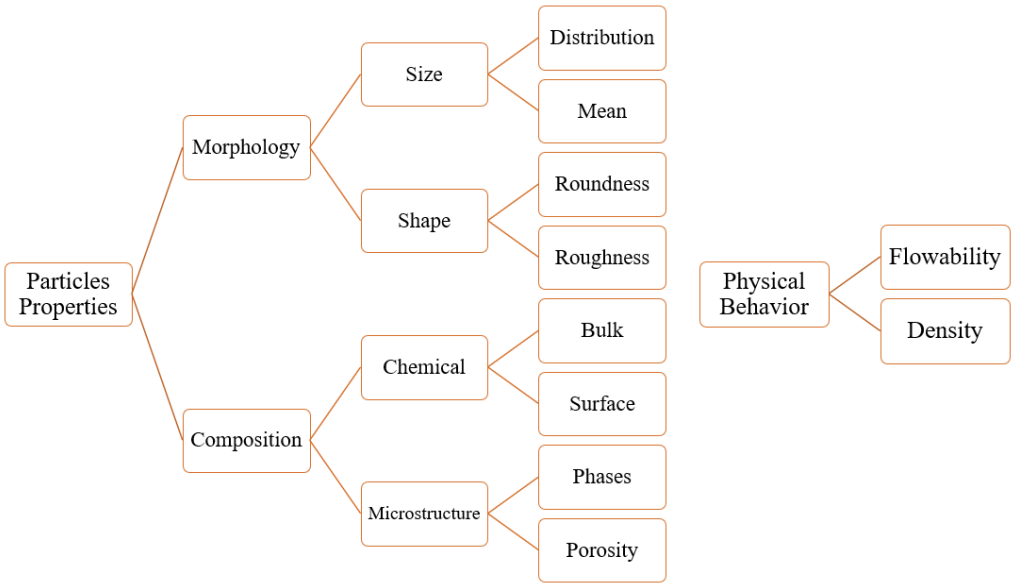

Figure 1.1. Highlights for the characterization of powders used in additive manufacturing [5]

Of course, repeatability of this quality is also critical. For this reason, it is known that many medical companies use virgin, that is, never used powder in each production. However, this is very costly increasing the amount of waste material. Thus, it is very important to collect and sieve the unused powder after a build is completed to reuse it in the coming jobs. Although it varies from equipment to equipment, an undeniable portion of the powders comes back from the process in powder form without being added to the main product. Throwing away so much metal powder without being reused is a huge financial loss. The subject of controlling the properties of these powders and reusing them in future productions is an area that needs to be investigated, and it is encountered by every unit that has engaged in additive manufacturing in academia and industry.

The aim of this thesis is to investigate the effects of powder reuse in 17-4 PH stainless steel processed by selective laser melting on the powder characteristics as well as built part properties. For this purpose, 10 consecutive productions were realized using exactly the same powder with no virgin powder additions. Various properties of the powder were examined and a set of tests were carried out on the final products. Tests performed on powders are density measurement, particle size distribution analysis, chemical composition analysis and flow rate measurements. At the same time, Archimedean density measurement, optical occupancy analysis, chemical composition measurement and surface roughness measurement were performed on the products obtained, and tensile test and hardness measurements were carried out in order to determine the mechanical properties of the parts. By examining the results of these tests, a correlation was tried to be made between the change in powder properties and the part properties obtained as a result of production.

This thesis consists of 5 titles in total. The title of the introduction is followed by CHAPTER 2, which includes the literature review. In this section, the general definition of additive manufacturing among its classification has been presented comparing its advantages and disadvantages. Selective Laser Melting has been detailed as well as 17-4 PH stainless steels A literature review on the effects of metal powder characteristics on the selective laser melting method is given, and metal

powder characterization methods encountered in past studies are mentioned. Finally, general metal powder reuse studies are summarized and then academic articles on 17-4 PH stainless steel powder reuse are summarized. CHAPTER 3 is the part where the experimental procedure of thesis experiments is explained. In this section, the properties of the main powder used are given and production planning is explained. Apparatuses designed for the tests are mentioned. In addition, test methods for both powders and the final parts obtained are also included in this section. CHAPTER 4 covers the results and comments after the experiments, the procedure of which is described. Finally, the closing and the planned future work are described in CHAPTER 5.

CHAPTER 2

LITERATURE REVIEW

In this chapter, the basic information underlying the additive manufacturing process is explained with the support of the literature. Information about the types of additive manufacturing is given and the method used in this thesis is emphasized and detailed literature review information is given. In addition, a section that contains in-depth information about the material used in the experiments is included in this chapter. Finally, a title including what kind of powder characterization techniques are used in similar studies in the literature is also included.

2.1 Additive Manufacturing

According to the definition made by American Society of Testing and Materials (ASTM), Additive Manufacturing (AM) combines materials layer by layer to obtain products from 3D model input. Names like additive fabrication, 3D printing, additive layer manufacturing and freeform fabrication are also used to denote additive manufacturing [2]. In accordance with the ASTM, additive manufacturing technologies are sorted into several categories (Table 1). Although they all share the principle used for selective modelling of layers, each category contains different operations [6].

Table 2.1 ASTM Categories of AM Technologies [2][6]

Binder Jetting	The liquid binding element is selectively deposited to combine with the powder material.	Metal Polymer Ceramic
Directed Energy Deposition	An energy source such as electron beam, plasma arc or laser is used to melt and combine the materials while they are being deposited.	Metal: powder and wire
Material Extrusion	Material is scattered selectively via a hole.	Polymer
Material Jetting	Droplets of the material from which the final product will be obtained are collected selectively.	Photopolymer Wax
Powder Bed Fusion	Certain areas of the powder bed are selectively melted and fused with thermal energy.	Metal Polymer Ceramic

Table 2.1 (cont'd)

Sheet Lamination	The final product is created by combining the materials in sheet form.	Hybrids Metal Ceramic
Vat Photopolymerization	By using light activated polymerization, photopolymer in liquid state which is in a barrel is cured selectively.	Photopolymer Ceramic

2.1.1 Advantages of Additive Manufacturing

There are many advantages of using additive manufacturing technology instead of conventional methods. The ability to create almost any complex shape is the biggest advantage of the additive manufacturing method. This capability is achieved through layer by layer production. Prototyping and modelling are the main areas where additive manufacturing technologies are most widely used. Moreover, additive manufacturing is used for short run prototype production. Also, it is used in small batch series production [7]. One of the other advantages is that the final product is produced directly and no extra material is lost. It becomes possible to produce parts with very complex geometries with less cost with additive manufacturing. It reduces the costs involved in product development activities because the need for fixtures developed specifically for the part is completely eliminated with this method. In this way, companies can be more efficient in their innovative progress. Another advantage is that the need for labor is minimized. Labor and repair costs are minimized [8].

2.1.2 Challenges of Additive Manufacturing

Although additive manufacturing is a groundbreaking technology, the application of the technology involves some difficulties. One of them is about size limits. Additive manufacturing devices can only produce parts as large as their volume allows. This means that parts of some sizes cannot be produced in a single production. For this reason, large parts must be produced in small segments and then assembled. This creates additional time and additional process requirement to reach the final product. In addition, additive manufacturing is a slower process than conventional manufacturing methods. Therefore, it is not efficient in terms of mass production. In addition, the expensiveness of additive manufacturing devices is one of the obstacles to this method. However, with the widespread use of 3D technology, these prices will also decrease [8].

2.2 Selective Laser Melting

The most widespread additive manufacturing procedure is named Selective Laser Melting (SLM). SLM is enhanced at the Fraunhofer Institute for Laser Technology ILT [9]. SLM appears to be the most miscellaneous operation when looking at the prospects of additive manufacturing. Engineering polymers, ceramics, metals and a broad variety of composites can be produced via SLM [10]. SLM is a method included in the powder bed additive manufacturing class. SLM permits the production of operational 3D parts based on CAD models. In this method, the powders are 100% melted. Subsequent metal powder layers are completely melted by exposure to high intensity laser beam and they become solid by melting on each other. After the whole process, parts with a density close to 100% are obtained. The best part is that generally there is no need for any post-production processes other than surface improvement processes [11]. SLM facilitates the fabrication of materials with complex shapes. Moreover, SLM creates parts that are coherent with the mechanical properties of conventional materials obtained through mass

production. In the production methods currently in use, some pre-production expenses are incurred. It is also a must to supply equipment specific to the part to be produced. For example, these demanding and time-consuming requirements must be fulfilled when it is desired to produce steels or alloys based on aluminum, titanium and nickel in series with identical properties. When it comes to production with SLM, none of these preparations is required [12]. Therefore, SLM saves both time and money. Today, the materials used in the SLM method are limited to a few. The reason for this is that the production parameters for each material are different from each other. The necessity of making separate parameter development studies for each material causes the range of materials used currently to be low. AISI 316L, Inconel 625, CoCr alloys, Ti-6Al-4V and 17-4 PH stainless steel can be given as examples to the materials used at the moment. Extensive studies are continuing in order to use the SLM process for other materials as well [1].

2.2.1 Principles of Selective Laser Melting

The SLM method includes several steps, from the preparation of CAD data to the separation of the final product from the production table. Before loading the CAD data into the SLM device, stereo lithography (STL) files of these data must be created with the help of a software. An example of this software is Magics. The reason for converting to STL format is that support structures of overhanging features can be created and slice data is generated for laser scanning of each layer. In the first step of the SLM process, metal powder is laid on the production table as a thin layer. Then, according to the data processed in the device, metal powders in selected areas are melted with a laser with high energy density. After the laser scanning of this layer is completed, the platform where the production table is located goes down as much as the layer thickness. Then, a new layer is laid on previous layer and the same process is repeated. The entire piece planned to be produced is completed in this way by advancing layer by layer.

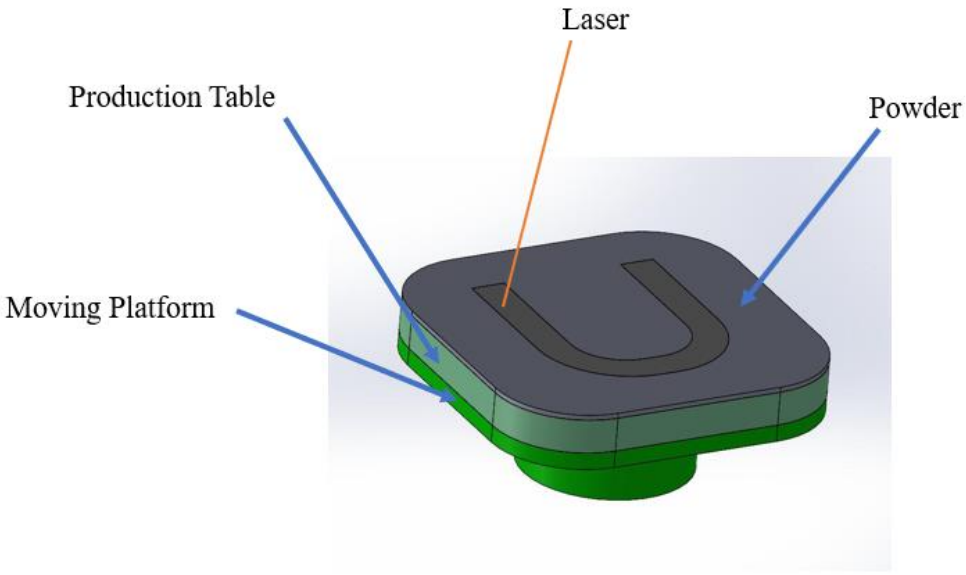

Figure 2.1. First layer of SLM process

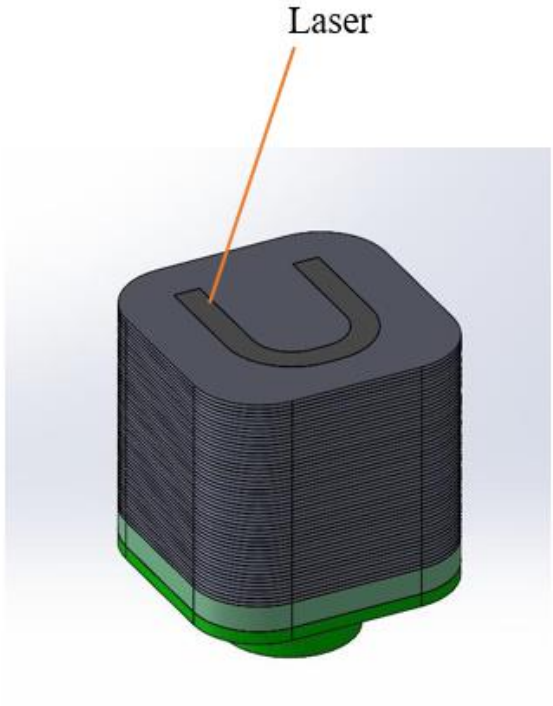

Figure 2.2. n^{th} layer of SLM process

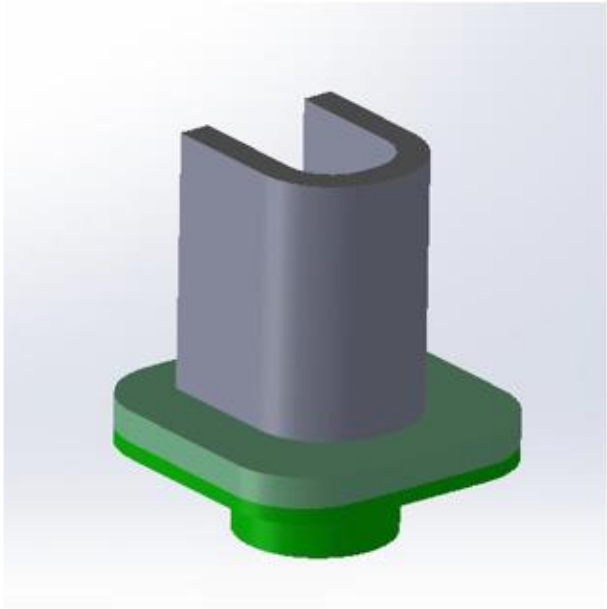

Figure 2.3. Powder free finished part obtained after the SLM process

In the SLM process, the laser power, scanning distance, scanning speed, layer thickness parameters are adjusted in such a way that each adjacent melt pools are fused and each layer is fused with the previous layer. After the laser scanning process is finished, the unmelted powders are removed from the production platform and the final product is separated from the production table manually or with the help of electrical discharge machining (EDM). In the SLM process, all processes are automated except for the preparation of the initial data and the separation of the last piece from the production table. Productions are generally carried out under nitrogen or argon gas. The purpose of this is to provide an inert environment in order to prevent oxidation of the heated metal part [13].

2.3 Information about Stainless Steels

Steels with at least 12% chromium content are generally referred to as stainless steel. The passive film formed on the surfaces of these materials gives stainless steels corrosion resistance and rust-free properties. The thin protective oxide layer formed on the metal surface gives the metal its stainless feature. If this passive layer is

broken, serious attacks occur in stainless steels. As a result, local based attacks such as pitting corrosion, inter-granular corrosion, crevice and stress corrosion cracking occur. Interest in stainless steels has grown tremendously over the last 37 years compared to other important metals (Table 2.2). Looking at the last 5 years, worldwide stainless steel production has increased by 34%. While stainless steel production is mostly carried out in China, India has ranked second in the last 2 years.

Table 2.2 Major metals' annual growth rate (from 1980 to 2017)

Metal	**Compound annual growth rate (%/year)**
Stainless Steel	5.39
Aluminium	3.90
Copper	2.67
Carbon Steel	2.35
Zinc	2.20
Lead	1.99
Average	2.44

Nickel was explored by Axel Fredrik Cronsted in 1751, molybdenum was explored by Carl Wilhelm Scheele in 1778 and Nicolas-Louis Vauquelin explored chromium in 1797. Eduard Maurer received a patent for austenitic stainless steel in 1912. The basic element of stainless steel is chromium. Even though the chromium element was found in 1797, stainless steel was produced after 115 years. Martensitic stainless steel was manufactured in 1913 by Henry Brearly. Elwood Haynes received a patent for ferritic stainless steel in 1919. Duplex stainless steel was produced for the first time in 1930. Almost 60% of stainless steels contain the element nickel. The role of

nickel in iron-chromium-carbon alloys is to stabilize the austenite phase. In other words, it is an austenite stabilizer.

2.3.1 Types of Stainless Steel

Stainless steels are generally classified as follows:

1. Austenitic,
2. Ferritic,
3. Martensitic,
4. Duplex,
5. Precipitation hardenable alloys.

2.3.1.1 Austenitic Stainless Steel

The largest of the stainless steel family are the austenitic stainless steels. This groups accounts for two-thirds of stainless steel production. Their microstructure is austenitic. This microstructure is obtained by alloying adequate nickel and/or manganese and nitrogen. In this way, the austenitic microstructure is preserved at all temperatures from sub-zero to the melting point. Since austenitic stainless steels have the same microstructure at all temperatures, they are not hardened by heat treatment. They are hardened by cold working limited to thin plate and small diameter bars. Having an austenitic microstructure gives this group of stainless steels excellent formability and weldability properties. In addition, this stainless steel is non-magnetic and shows ductility at sub-zero temperatures.

2.3.1.2 Ferritic Stainless Steel

The microstructure of ferritic stainless steels consists of ferrite. Due to the chromium content, this microstructure is preserved at all temperatures. Therefore, they are not hardened by heat treatment. They do not achieve as much hardening by cold working

as with austenitic stainless steels. Ferritic stainless steels are magnetic. They are not suitable for welding. This is because grain growth is observed in the heat affected zone and the ductility value decreases as a result of this growth. This causes cracks. Increasing chromium and molybdenum elements means increasing corrosion resistance. However, this high alloying causes brittle phases to precipitate during welding. This prevents ferritic stainless steels to be used in very thin thicknesses.

2.3.1.3 Martensitic Stainless Steel

Many important materials, including stainless tool steel, stainless engineering steel and creep resistant steel, consist of martensitic stainless steels. Because this type of stainless steel offers a multitude of properties. Martensitic stainless steels comprise 12-15% chromium element, 0.1-1% carbon element and 0.2-1% molybdenum element. They do not contain nickel element. This combination of elements indicates ferro magnetism. The magnetic features of martensitic stainless steels vary according to the strength of the adopted magnetic field. If this type of stainless steel is magnetized during hardening, they always have permanent magnetic characteristics.

2.3.1.4 Duplex Stainless Steel

Stainless steels that contain both austenite and ferrite phases in their microstructure are called duplex stainless steels. They contain 19-32% chromium element, a small amount of nickel element and up to 5% molybdenum element. The nickel content they contain is less than austenitic stainless steels. They are twice as strong as austenitic stainless steels. They have high corrosion resistance and strength thanks to their dual microstructure.

2.3.1.5 Precipitation Hardening (PH) Stainless Steel

As a result of the rapid development of the aviation industry since 1940, precipitation hardened stainless steels have emerged in order to meet the increasing material demand. Having a corrosion resistance comparable to austenitic stainless steel, precipitation hardened stainless steels can have much greater strength than other martensitic stainless steels by precipitation hardening. Elements that enable precipitation hardening in martensitic stainless steels are mainly copper and niobium. PH stainless steels are highly preferred in marine industry, aviation industry, medical apparatus and nuclear reactor components. The main reasons why they are preferred in these areas are their high tensile strength, high fracture toughness and high corrosion resistance. The temperatures at which they can be used are below 300°C. The machinability of PH stainless steels is not very good. This is because they have high strength and high hardness. Due to these features, long and difficult processes are passed while this type of stainless steel is given the desired shape. For these reasons, PH stainless steels are in the group of materials that are difficult to produce with conventional processing methods. At this point, additive manufacturing emerges as a new method that enables the production of PH stainless steel parts that must have complex shapes [14]. 17-4 precipitation hardening stainless steel is the most popular of this type and contains 17% chromium element and 4% nickel element [15].

2.3.1.5.1 17-4 Precipitation Hardening Stainless Steel

17-4 precipitation hardening stainless steel is a martensitic stainless steel but it contains approximately 3% copper element and its strength is increased as a result of the precipitation of copper particles in the martensite matrix [16]. The chemical composition of the 17-4 precipitation hardening stainless steel according to the AMS 5643 standard is given in Table 2.3.

Table 2.3 Chemical composition of 17-4 precipitation hardening stainless steel given in wt%

Element	***min***	***max***
Carbon	-	0.07
Manganese	-	1.00
Silicon	-	1.00
Phosphorus	-	0.040
Sulfur	-	0.030
Chromium	15.00	17.50
Nickel	3.00	5.00
Columbium	5xC	0.45
Copper	3.00	5.00
Molybdenum	-	0.50

17-4 PH stainless steel is the most preferred precipitation hardening stainless steel in additive manufacturing to date. The reason for this can be listed as follows [17]:

- Good printability,
- Various field of application
- High strength
- High corrosion resistance

In order to provide properties such as mechanical properties and corrosion resistance, 17-4 PH stainless steels generally need to be heat treated. To obtain the desired hardness and strength, aging heat treatment is applied to this material at temperatures in the range of 480-620°C. Optimal hardness and strength properties are obtained by the formation of nanometric copper precipitates [18].

2.3.1.5.1.1 Microstructure of 17-4 PH Stainless Steel

The microstructure of 17-4 PH stainless steel produced by conventional methods is martensitic. However, when it comes to the 17-4 PH stainless steel produced by additive manufacturing, there are many reports in the literature about the microstructure formed as a result of the production. It has been reported that the microstructure of 17-4 PH stainless steel produced by laser powder bed fusion under argon atmosphere has a martensitic structure with a small amount of retained austenite [1]. In another study, it was stated that the 17-4 PH stainless steel produced by the same method had a ferritic structure with large grain size and the grains were elongated in the direction of production [19]. The metallurgy of this steel was studied in terms of solidification and cooling to explain the different microstructures resulting from additive manufacturing parts. When there is a cooling in the equilibrium state, the 17-4 PH stainless steel first solidifies from the liquid state to the delta ferrite phase. Then, the delta ferrite phase transforms into austenite during cooling due to solid state diffusion. Afterwards, austenite transforms into martensite at the stage of coming from 132°C to room temperature. All this explains the reason why the microstructure of the conventional 17-4 PH stainless steel is martensitic. Due to the high cooling rate in the laser powder bed melting process, transformations in equilibrium conditions are not possible. Since the cooling is very fast, the delta ferrite phase does not have enough time to transform into austenite. Thus, the microstructure remains in delta ferritic structure at room temperature. That is, the transition from delta ferrite to austenite is related to how long ferrite can stay in the region where austenite is stable. In the literature, it is mentioned that the time spent in the region where austenite is stable depends on the chemical composition of the starting powders. Cr_{eq}/Ni_{eq} ratio is important in understanding the solidification behavior of stainless steel. As this ratio decreases, the time spent in the region where austenite is stable increases. According to the information obtained from the literature, when this ratio is higher than 1.5, the delta ferrite phase is stable at room temperature [18]. It was observed that a martensitic microstructure was obtained

when solutionizing heat treatment was applied to 17-4 PH stainless steel produced via SLM [20].

2.3.1.5.1.2 Metal Powder Production

In order to produce 17-4 PH stainless steel products with the SLM method, the powders of this material must first be fed into the SLM device. Four different ways are used in the production of metal powders.

1. Chemically production
2. Electrolysis
3. Mechanically production
4. Atomization

The most widely used method for the production of powders planned to be used in additive manufacturing is the gas atomization method. This method is carried out in an inert gas environment. The liquid metal is atomized by a high energy gas flow. Then the atomized liquid metal turns into spherical droplets. They then arrive in solid form when cooled to a temperature below their melting point. These solid particles are separated according to their size by sieving method.

2.4 Effects of Metal Powder Characteristics on Selective Laser Melting Process

In additive manufacturing processes, the quality of the end product is highly dependent on the quality of the powders loaded in the first place. There are a number of characteristics that determine the quality of powders. These characteristic features are listed as follows:

- Particle shape, morphology
- Humidity
- Particle size distribution
- Flowability

2.4.1 Effects of Powder Shape

The defects often encountered in additive manufacturing powders are their irregular shapes. Elongated powders, satellite formation or porous powders are examples of these. Such defects affect the flow properties of powders. Powders with a spherical shape are better in terms of good flow properties. In addition, powders with this shape play an important role in obtaining more regular powder layers. Large voids or gas filled voids in the powder affect the material properties. At the same time, the stacking density of the powders also depends on the shapes of the powders.

2.4.2 Effects of Humidity

More than one molecular layer can form on the particle surface, which affects the flow properties of the powders. Increasing the interactions between powders reduces flowability. Moisture in the powders causes a porous product to form.

2.4.3 Effects of Particle Size Distribution

The maximum size of the powders is the biggest factor in deciding the minimum layer thickness. A balanced particle size distribution positively affects the packing density. This is because small particles fill small voids. Small powders are light and escape easily from the production area. The use of metal powders with a small powders size and a narrow powder size distribution causes the melt pools formed during laser melting to be more uniform. This enables higher density parts to be produced at the end of the process.

2.4.4 Effects of Flowability

Changes in other characteristic properties of powders affect the flowability properties of powders. Flowability directly affects layer deposition and layer quality. The formation of homogeneous layers depends on the flowability of the powders [21].

2.4.5 Methods Used in Characterization of Additive Manufacturing Powders

The consistency of the properties of the powders used in additive manufacturing is of great importance in terms of producing the same quality of metal parts produced in every production. For example, metal powders used in additive manufacturing should be spherical and the particle size distribution should be adjusted to achieve the appropriate packing behavior. The reason for these requirements is to obtain final products with a density close to 100% with the desired mechanical properties. Morphology, density, flow properties and chemical composition are also counted among other powder characteristics. There are several methods by which additive manufacturing powders are tested to measure these properties. There are several reasons for using these methods. First of all, these methods are used in deciding the variability between samples of powders produced by the same production. Furthermore, these methods are used to determine the effect of recycling on powder properties. The use of these methods is critical to correlate the mechanical properties of parts made with additive manufacturing with the properties of additive manufacturing powder. For example, Slotwinski et al. characterized two different metal powders in a study. Table 2.4 summarizes which methods they used to measure powder properties [22].

Table 2.4 Powder characterization methods

Characteristic Feature	***Method***
Powder Elemental Composition	Energy Dispersive Elemental Analysis
Powder Morphology	Scanning Electron Microscopy
Powder Size and Morphology	X-Ray Computed Tomography
Density of Powders	Helium Pycnometry
Powder Surface Molecular/Chemical Composition	X-Ray Photospectroscopy
Powder Size Distribution	Laser Diffraction
Powder Crystalline Phases	X-Ray Diffraction

Pleass and Jothi performed characterization tests on Inconel 625 powders in their study and examined the effects of powder characteristics on parts produced with additive manufacturing. The methods used in this study are summarized in Table 2.5 [23].

Table 2.5 Powder characterization methods

Characteristic Feature	***Method***
Chemical Composition	Inductive Coupled Plasma Atomic Emission Spectroscopy (ICP-AES)
Particle Size Distribution	Laser Diffraction
Powder Flowability	Carney Flow Test

Lutter-Günther et al. studied the effect of AlSi10Mg powders on additive production. The characterization methods used in this study are summarized in Table 2.6 [24].

Table 2.6 Powder characterization methods

Characteristic Feature	***Method***
Particle Size Distribution and Morphology	Scanning Electron Microscope (SEM)
Oxygen Content	Inert Gas Fusion (using infrared detector cell)
Oxide Layer Thickness	X-Ray Photoelectron Spectroscopy (XPS) and Sputtering
Alloy Composition	Inductively Coupled Plasma Optical Emission Spectrometry (ICP-OES)

2.5 Studies on the Reuse of Powders

It is necessary to look at what kind of experiments are carried out with which materials related to powder recycling. For example, Asgari et al. conducted a study about the microstructure and mechanical properties of unused and recycled Al-Si-10Mg powders. The recycled powder size increases by 12 % when compared to the unused powder. However, recycling did not indicate any important change in the microstructure and tensile properties of the produced parts [25]. Another study is as follows. Jelis et al. carried out a parallel study on 4340 steel and notified the presence of high oxygen content in reused powders. An important change in the ultimate tensile strength is introduced by the samples produced with reused powder. However, these studies concentrated on a single build cycle [26]. Maamoun et al. analyzed unused and reused Al-Si-10Mg powder particles after several cycles and did not state any primary change in powder morphologies. In addition, no primary

difference in density, microstructure and PSD were beholden in parts produced using unused and reused powders [27]. Gruber et al. studied unused and reused Inconel 718 powders and manufactured parts after 14 build cycles and indicated a higher content of Al-rich oxide particulates. Surface morphology was slightly changed [28]. Terrassa et al. performed a study about the influence of powder reusing on 316L stainless steel using direct energy deposition (DED) systems. It is well proved that a wider powder distribution ends up with a reduced porosity in manufactured parts [29]. And, it is straight known that porosity influences mechanical properties and part trustworthiness [30]. Because of too much recycling, degradation of powders takes place and the existence of larger particles influences the particle distribution, which eventuates in a higher porosity in manufactured parts. In this study, a swell in average particle size and oxygen content was found. Yet, they did not examine any important change in the properties of manufactured parts [31]. Tang et al. also conducted an examination about a detailed powder recycling on electron beam melting (EBM) of Ti-6Al-4V. A change in powder shape and distribution is indicated. The manufactured parts also signalized no measurable change in mechanical properties [32]. Looking at all these studies in the literature, it can be said that the response of each material to powder recycling is different. Therefore, it is essential to perform these studies separately for each material.

2.6 Studies on the Reuse of Powders Specific to 17-4 PH SS Powders

17-4 PH SS is a highly preferred material because it contains many desirable features such as high tensile strength, high toughness and high corrosion resistance [33][34]. For this reason, this material seems to be very suitable for use in many structural parts in aviation applications. Considering the complex geometries of parts in aerospace applications, the SLM method is an excellent way to produce these parts. Due to its ease of printing and high properties, 17-4 PH SS is a good choice in terms of being preferred as the material to be produced with SLM [35]. For this reason, it is necessary to work on the reuse of 17-4 PH SS powder material in the SLM process.

Zapico et al. carried out a study by using 17-4 PH SS powder. In this study, 17-4 PH SS powder used in SLM process is characterized in three different aspects: (i) original state (or unused state), (ii) after using 10 times and (iii) 20 times, in turn. The reusing process comes out of recovering the powder that is not molten by implementing vacuum and sieving it to reload the powder chamber in the SLM machine. The three aspects of the powder were characterized morphologically, chemically, and microstructurally. Many powder samples were examined with an optical microscope and powder shape analysis was performed. Considering the results, serious changes were observed in the shapes of the powders that were reused 20 times. They evaluated that this change in shape would have a negative effect on the mechanical properties of the final part obtained [36]. Ahmed et al. performed a study about 17-4 PH SS powder recycling. The information found is as follows. The powder analysis indicates that as concerns the unused powder, the irregular shaped powders swell in the feedstock with reusing. The power after print 10 showed a minor increase in particle size (D10: 3 %, D50: 2.8 %, and D90: 3 %.) when compared to print 1. Reusing of powder also influence the sphericity of particles. As a result, the print 10 powders' basic flowability energy was seen to swell by 35 % compared to unused powder [37]. Slotwinski et al. indicates that XPS showed important differences in the surface chemistry of the stainless steel sieve residue particles and the unused 17-4 PH SS powders. Spherical powders are debated best for additive manufacturing implementations because they end up the best flowability and powder-bed jamming resulting in non-porous parts [38]. The progress in the size of the powders and their shape not only influences the morphologic characteristics of the particles, but also influence the standard of the printed parts. This can be clarified by a decrease in the powder fluidity [39], which is influenced by the agglomeration of small powders [40] and by the swell of irregularity in the powder's shape because of the increase of cohesive forces between them [41].

CHAPTER 3

METHODOLOGY

Under this title, the powder material used in this thesis is introduced and the additive manufacturing procedure applied to monitor the recycling of powders is included. Afterwards, the preparation procedure of the powder samples to be used in powder characterization tests, the powder properties to be characterized and the equipments used for these tests are given in detail. Finally, the tests performed on the parts obtained as a result of the productions are included in the last heading of this section.

3.1 Powder Material

The material used in the experiments of this thesis is 17-4 precipitation hardening (PH) stainless steel (SS) powder. It is known that these powders used are produced by gas atomization method. The SEM image of the powders taken from the supplier are shown in the figure below. In general, the powders have a spherical shape but various deformations are also observed (eg. satellization, agglomerated powders, etc.). The standard composition of the powders is given in Table 3.1 (Carpenter Additive). It is known that the particle size distribution of the powders is between 15-45 microns.

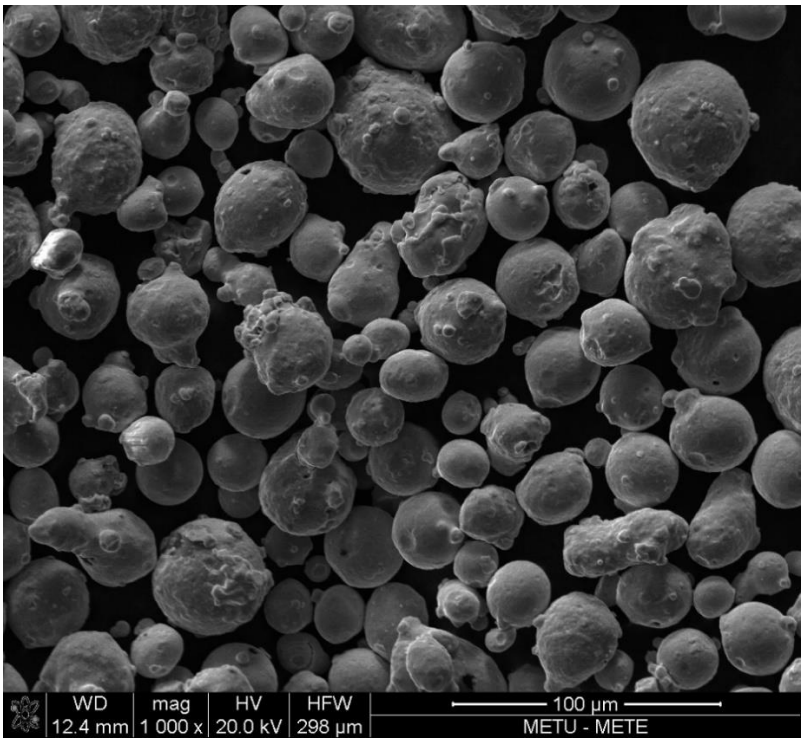

Figure 3.1. SEM image of 17-4 PH SS powders

Table 3.1 Chemical composition of 17-4 PH SS powder given in wt%

Iron	Balance
Nickel	3.00-5.00
Niobium+Tantalum	0.15-0.45
Carbon	0.070 max.
Chromium	15.00-17.50
Manganese	1.00 max
Nitrogen	0.10 max.
Phosphorus	0.040 max.
Copper	3.00-5.00
Silicon	1.00 max.
Oxygen	0.10 max.
Sulfur	0.030 max.

3.2 Production Plan

In order to see the effect of repeated use of 17-4 PH SS powders on the powders and final production parts in the SLM process, some additive manufacturing productions are planned. Productions were carried out on the Renishaw AM400 brand device. Since the interior volume of the additive manufacturing device where the SLM process is carried out is large and a large amount of powder material must be spent for powder reuse experiments, it was decided to use the reduced build volume (RBV) unit of the device. By using this unit, less amount of powder was used and productions were carried out without affecting the main production plan of the company which supports the realization of the productions required for the formation of this thesis.

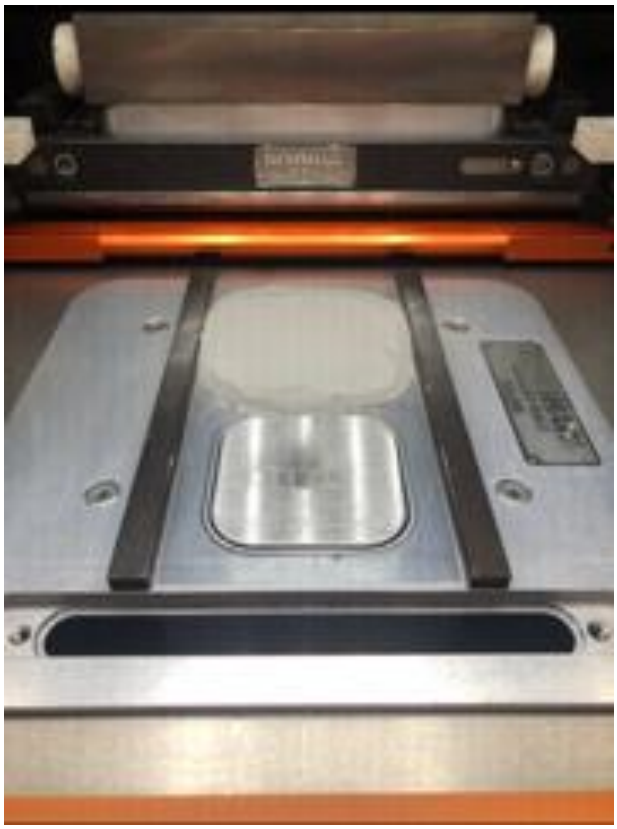

Figure 3.2. Renishaw RBV unit

Before first production, approximately 2973 grams of powder was filled in the RBV unit to completely fill the powder chamber. During the successive productions, the powders were sieved with a 45 microns hand sieve at the end of each production and then the sieved powders were loaded back into the chamber. Since the amount of powder used was low, using a hand sieve instead of the sieve of the additive manufacturing device had allowed a more controlled sieving process. It is useful to state that no unused powder was added to the chamber during the productions and that the productions were carried out by using the same powders all the time.

Figure 3.3. Hand sieve equipment (45 microns)

A total of 10 productions were planned and tensile test specimens were produced for the purpose of mechanical property control in the 1st, 5th and 10th productions. In addition to the tensile test specimens, thin block pieces were also produced along the production height in order to examine the final product features. Several requirements have been considered during decision making phase of the part to be produced in intermediate productions. These requirements can be listed as follows. First of all, since the aim is to successfully complete the production of 10 with the same powders, as little powder as possible should be spent on production in intermediate productions. At the same time, the surface area of the workpiece must be high so that most of the powders can be affected by the laser. Based on these requirements, it was decided that the most appropriate product to be selected should

be a support structure. By using the support structure, a piece with a small volume but a large surface area was obtained. Thus, a small amount of powder was lost in intermediate productions and as many powder particles as possible were exposed to the laser.

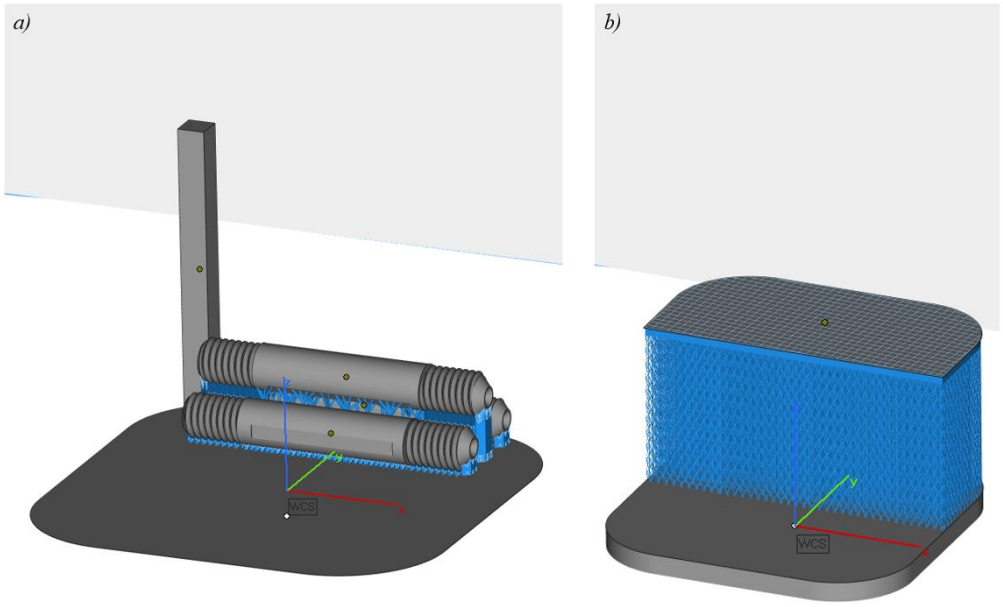

Figure 3.4. Parts produced in a) 1st, 5th and 10th and b) intermediate productions

The production parameters that are currently used for the production of 17-4 PH SS in the company were used. Parameters can be seen in Table 3.2. Parts were produced with a layer thickness of 30 microns. 67 degrees of rotation was made on each layer in the productions. The reason for this rotation is to reduce the residual stress as much as possible. With each stroke of the laser on the powder layer, the powders melt and fuse and cool by transmitting the heat to the layers below. This happens in milliseconds. Formed new solid layer is constrained by the solid material below. As a result, residual stress is created. Each layer is scanned by rotating 67 degrees in order not to cause constant tension in the same place. Meander was used as the scanning strategy.

Table 3.2 Parameters used in productions

Power (P)	200 Watt
Point Distance (PD)	110 μm
Hatch Distance (HD)	110 μm
Exposure Time (ET)	142 μs
Layer Thickness (LT)	30 μm

3.3 Preparation of Samples

The design of the tensile test specimens produced by additive manufacturing, the apparatus used to prepare powder samples, heat treatment coupons preparation steps and metallographic sample preparation stages are explained in detail under this subheading.

3.3.1 Tensile Test Specimen Design

Tensile test specimens were produced in order to see the effects of the reuse of powders on the mechanical properties of the printed parts in the 1^{st}, 5^{th} and 10^{th} productions. The dimensions of the tensile test specimens of materials are determined by the standards. For metal materials this standard is ASTM E8m [42]. The depth and width of the production table of the RBV unit are both 78 millimeters. It can produce up to a maximum height of 55 millimeters. There is no tensile test specimen size that can be produced with the production volume of the RBV unit in the ASTM E8m standard. The RBV unit remains small for this operation. For this reason, it was necessary to design a tensile test specimen so that it can be produced in accordance with the standard inside the RBV unit. The details of the design made for this purpose are shared in Figure 3.5.

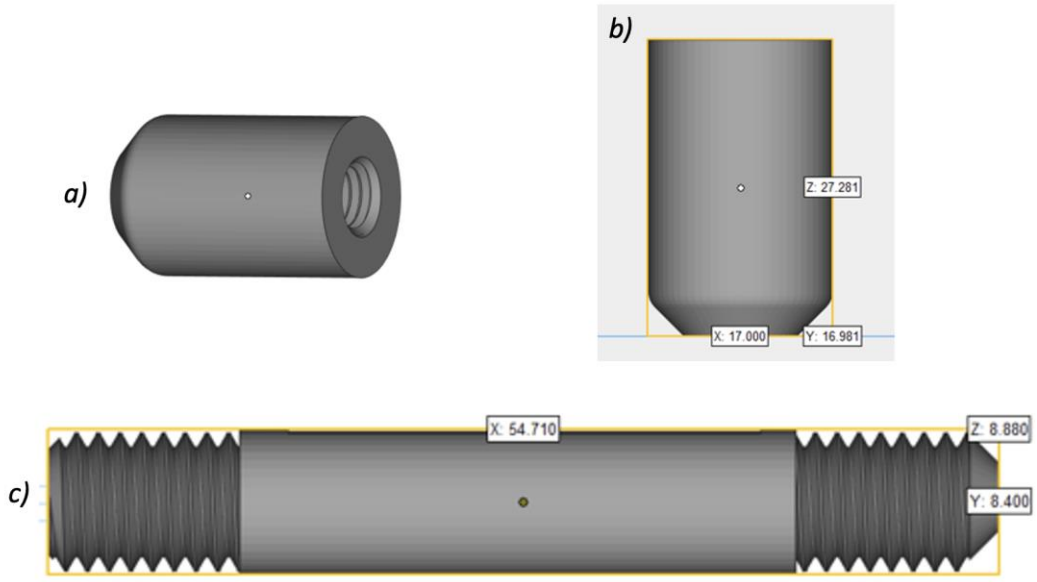

Figure 3.5. Designed tensile test specimen a) part that attached to the tensile test equipment b) dimensions of part that attached to the tensile test equipment and c) body of tensile test specimen with dimensions

The body of the tensile test specimen was manufactured in the RBV unit. The gauge length was produced in accordance with the standard and it was decided to make the diameter suitable for the standard with the turning process by keeping the diameter excessive during production. As normally the entire length of the specimen remains long for production within the unit, parts of the specimen that attach to the tensile test equipment on both sides of the specimen were produced separately. From the part shown in Figure 3.5 (a), two pieces were produced for each specimen, the inner part of these parts was opened with a guide and screwed to the body produced in the unit (Figure 3.5 (c)). This resulted in a tensile test specimen conforming to the standard. Tensile test specimen was obtained in accordance with the dimensions of the 4-diameter tensile test specimen in ASTM E8M standard.

3.3.2 Powder Sample Preparation

At the beginning of the experiments, a sample was taken from the powder that was never used. Then, powder samples were taken after 10^{th} productions in order to observe the changes in the properties of the powders as they were reused. It is critical that the powder samples which are planned to be used in tests are formed correctly. Powder samples were created in accordance with the standards so that these powder samples that are used small amounts can reliably represent all the powders in question. The sampling steps of metal powders are described in ASTM B215 standard [43]. Accordingly, a number of steps were followed in powder sample formation. First of all, a sampling apparatus was designed so that powder samples can be taken from the container in which the powders are located from any height. The apparatus consists of 2 parts. The drawing of the design is shown in Figure 3.6.

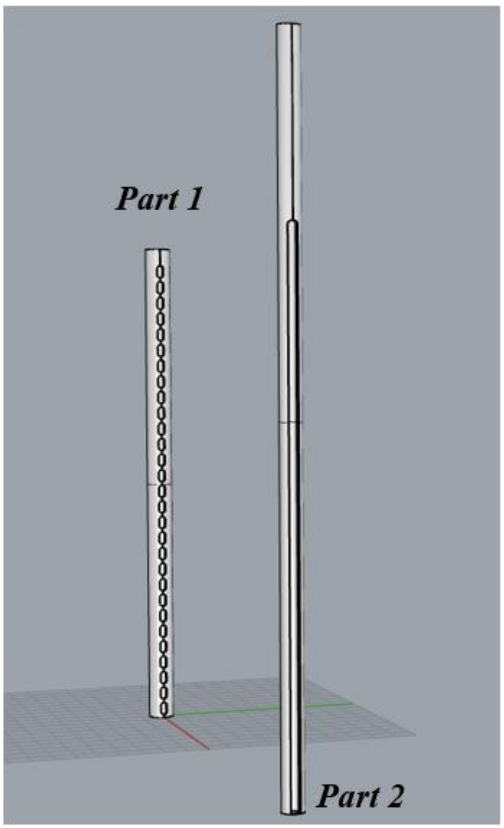

Figure 3.6. Sampling apparatus design

The apparatus parts were obtained from the tubular material by processing with a molding milling cutter. The production steps of the apparatus are shown in the Figure 3.7.

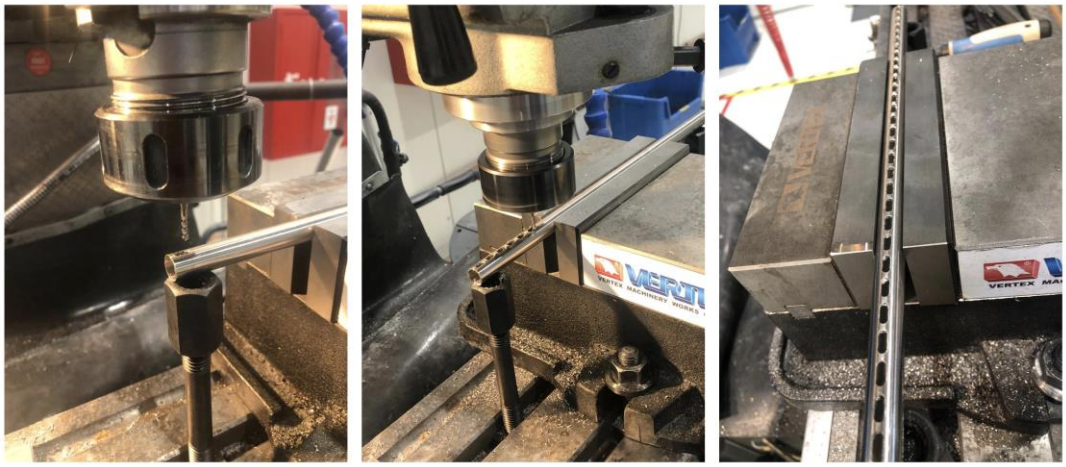

Figure 3.7. Production steps of sampling apparatus

A piece of the same material was cut and welded to the lower part of part 1 and it was closed with a single end. The part 2 which has a cylindrical all-round opening was placed in the part 1. This apparatus was immersed in the container with powder and powder samples were taken from every height of the container.

Figure 3.8. Sampling of powders by using designed apparatus

This process was repeated by immersing the container from 3 different places and the collected powders were loaded into the powder splitter shown Figure 3.9. There are total of 12 channels in this equipment, 6 to the right and 6 to the left. The powders filled from the top of the splitter were passed through these channels and were collected in 2 powder sample collection boxes at the bottom. The powder collected in a box was taken and divided into two by passing it through splitter again. This separation process was continued until the required amount of powder sample was obtained.

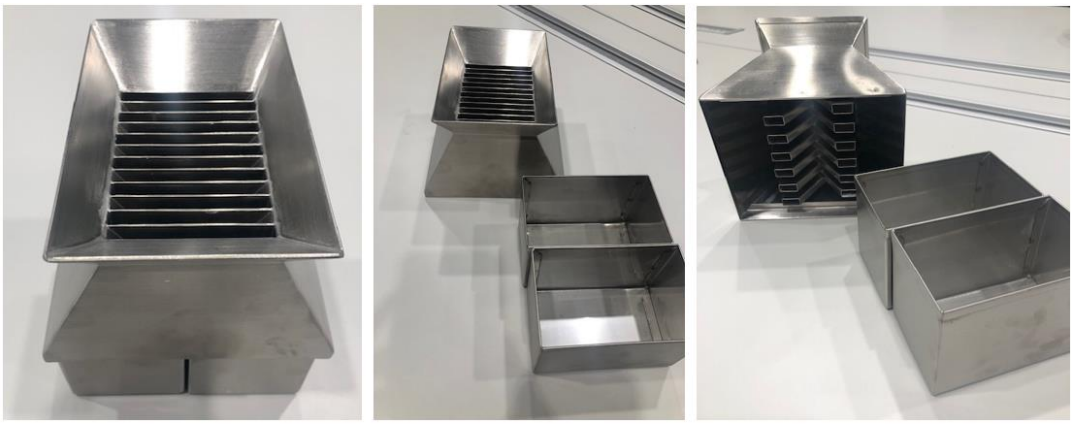

Figure 3.9. Powder splitter

3.3.3 Heat Treatment Coupon Preparation

After the tensile tests in the as-built condition, the ends of the tensile test specimens were cut off and heat treatment samples were formed.

Figure 3.10. The ends of the tensile test specimen

The dimensions of the heat treatment coupons are shown in Figure 3.11 below.

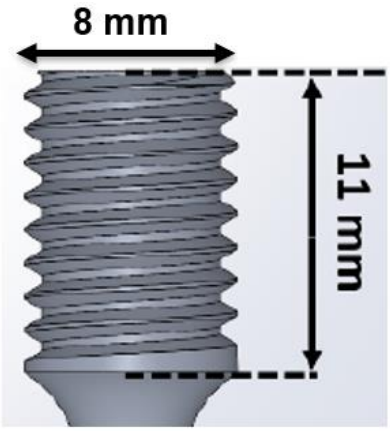

Figure 3.11. Dimensions of the heat treatment coupons

In order to be used in the evaluation of the changes that the 17-4 PH stainless steel material produced by SLM method will show as a result of the heat treatment, heat treatment coupons were also created from the condition of the same material produced by conventional methods. First, a 20 mm thick piece of 150 mm diameter billet was cut with a band saw.

Figure 3.12. 150 mm diameter 17-4 PH SS billet

Then, 20 mm thick piece was attached to the electrical discharge machining (EDM) device and a 100 mm long cylinder with 8 mm diameter was cut from it. Afterwards, this cylinder piece was sliced in an abrasive cutting device with a length of 11 mm in order to have similar dimensions with the additive manufacturing heat treatment samples.

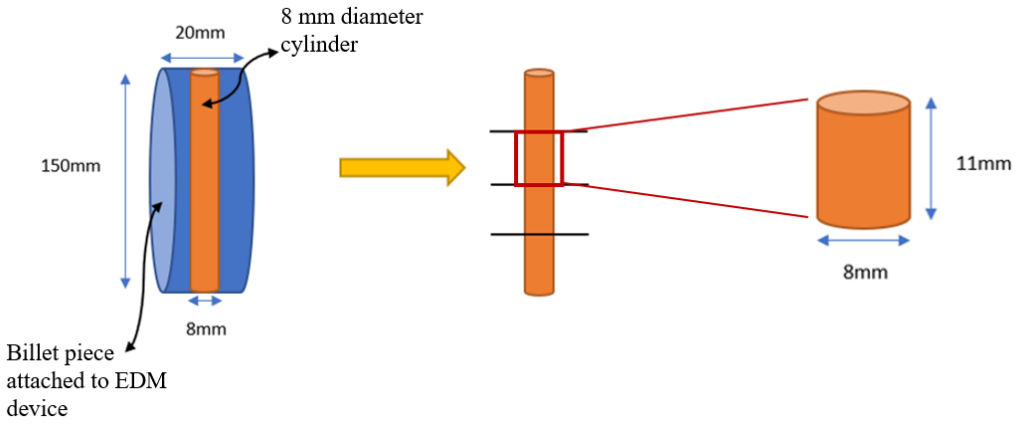

Figure 3.13. Heat treatment coupon production from conventional material

3.3.4 Metallographic Sample Preparation

Metallographic sample preparation was carried out in order to accurately measure the hardness of the produced parts, examine the porosities and investigate the microstructure before and after heat treatment with an optical microscope. For as-built hardness testing, the block piece obtained from the productions was cut and placed in bakelite. Afterwards, the surface of the sample was brightened by using automatic grinding and polishing equipment. For microstructural investigations, after mounting, grinding and polishing procedures, the samples were etched for 30 seconds using Fry's reagent. Microstructural examination was carried out on the surfaces of the parts parallel to production direction.

3.4 Characterization of Powders

The powders taken from the unused powder and powders removed from the production platform at the end of the 10^{th} productions, in accordance with the sampling rules, were subjected to a number of tests in order to see the effect of reuse. The tests are described in order below.

3.4.1 Morphology

Microscopic images of the powders were taken to control the shape changes and agglomeration of the powders as they were reused. Scanning electron microscopy (SEM) was used in order to see the powders' shape. SEM allows the visualization of powder particles at high zooms and determination of their chemical composition. It acquires an image by scanning the sample surface with a focused beam of electrons. Electrons interact with atoms in the sample, producing different signals that contain information about the topography and composition on the sample surface. SEM images were obtained from NanoSEM 430 microscope.

3.4.2 Chemical Composition Measurements

The chemical composition of the powders was measured by inductively coupled plasma optical emission spectrometry (ICP-OES). Apart from this method, a Leco brand device was used to check the oxygen and carbon content of the powders. Measurements were carried out in accordance with the ASTM E1019-11 standard [44]. Eltra brand device was used for carbon and sulphur analysis. Measurements were carried out in accordance with the ASTM E1941 standard [45].

3.4.2.1 ICP-OES

Inductively coupled plasma optical emission spectrometry (ICP-OES) is an analytical technique for the detection of chemical elements. It is a type of emission spectroscopy that uses induction coupled plasma to produce excited atoms and ions that emit electromagnetic radiation at wavelengths characteristics of a given element. It is a flame technique with a flame temperature between 6000 and 10000 K. The resulting emission intensity is an indication of the concentration of the element in the sample. ICP-OES measurements made within the scope of this thesis were carried out in accordance with the ASTM E1479 standard [46].

3.4.3 Powder Density Measurements

Within the scope of this thesis, three different density values of the powders were measured. These are listed below.

1. True Density
2. Bulk Density
3. Tapped Density

3.4.3.1 True Density Measurements

Gas pycnometry is the name of the method that determines true density of the metal powders. It is a non-destructive method. This method uses gas displacement in order to measure volume of the powders exactly. By this way, gas pycnometry becomes ideal for measuring true density. In this study, Anton Paar brand Ultrapyc5000 model was used in order to measure true densities of powders. Helium was used as filling gas.

Figure 3.14. Anton Paar brand Ultrapyc5000 model device

3.4.3.2 Bulk Density Measurements

Bulk density, also called apparent density, is the value found by the ratio of the mass of many powder particles to the total volume they occupy. The bulk density values were measured using a Hall flowmeter. The measurements were carried out in accordance with the ASTM B212 standard [47].

3.4.3.3 Tapped Density Measurements

The density value found by dividing the mass of multiple powder particles by the volume obtained by tapping these powders is called tapped density. The tapped density values were measured using a tapped density equipment. The measurements were carried out in accordance with the ASTM B527 standard [48].

3.4.4 Determination of Powder Size and Shape by Dynamic Image Analysis

Dynamic image analysis is a method that enables determination of particle size and shape with a camera with high speed and dimensional resolution with free falling and moving powders. The works were carried out with Microtrac brand Camsizer X2 model equipment.

Figure 3.15. Microtrac brand Camsizer X2 model equipment

3.4.5 Flow Characteristics

Changes in the properties of powders directly affect the flow properties. Therefore, the flow properties of the powders had to be examined within the scope of this study. Powder flow rate was measured in second per 50 gram in accordance with ASTM B-213 standard [49]. Flow rate values were measured using a Hall flowmeter.

3.5 Characterization of the Final Parts

The final parts manufactured at the 1st, 5th and 10th productions were subjected to a number of tests in order to see the effect of reuse of powders. In order to detect the changes in the mechanical properties of the final product as the production is made with reused powders, 3 tensile test specimens were produced in these steps. At the same time, a piece of rod was produced along the production height for density, hardness and surface roughness measurements, porosity observations and EDS analysis. Also, coupons were obtained from the ends of the tensile test specimens and heat treatment was applied to these coupons. The tests are described in order below.

3.5.1 Density Measurements

The density of the obtained parts is an important output that should be followed in the additive manufacturing process. Mettler Toledo brand device was used for density measurements. The device makes measurements based on the Archimedes principle. Archimedes principle allows the density to be calculated by using the weight difference in the air and auxiliary liquid (water, alcohol, etc.) of the piece to be measured. It is one of the fastest and low standard deviation methods.

3.5.2 Optical Occupancy Analysis

Optical occupancy test includes examining the section taken from a produced sample under the microscope and calculating the percent occupancy rate of the part by using the contrast difference. For this purpose, ImageJ image analysis program was used. This method is not based on a theoretical density, it allows to directly reach the percent occupancy rate.

3.5.3 Surface Roughness Measurements

Measurements were carried out in order to examine the effect of the changes that occur as a result of the reuse of the powders on the surface roughness of the obtained part. For this purpose, Mitutoyo brand SJ301 model surface roughness measuring device was used. Measurements were taken from 3 different points of the samples and their averages were calculated.

3.5.4 Hardness Measurements

The hardness of the obtained parts was measured from 5 different points. Emcotest brand Durascan model equipment were used for these measurements. Measurements were taken along the production direction. Hardness measurements were taken with a Vickers tip using HV1 and then converted to the corresponding Rockwell C value.

3.5.5 Tensile Test

In order to examine the change in mechanical properties as the powders are reused, 3 tensile test specimens were included in the 1^{st}, 5^{th} and 10^{th} productions. These specimens were then subjected to a tensile test. As a result of the test, yield, ultimate tensile strength and elongation percentage values of the material were obtained. Instron brand 5500R model tensile tester was used for this purpose.

3.5.5.1 Fracture Surface Examination

Scanning electron microscopy (SEM) was used in order to examine fracture surfaces. NanoSEM 430 microscope was utilized for this purpose.

3.5.6 Chemical Composition Analysis

Scanning electron microscopy (SEM) accompanied by energy dispersive elemental analysis (EDS) was used in order to measure the final parts' chemical composition. EDS analysis is performed by sending a scanning electron beam onto the sample. The emitted x-rays are detected by electronic sensors. The obtained data creates peaks on the computer monitor and elemental analysis is done. Chemical composition data were obtained from NanoSEM 430 microscope.

3.5.7 Heat Treatment

Various heat treatment procedures were applied to the parts obtained from the first production with unused powder and the last production, the 10th production, in order to control whether there was a change in the reactions of the parts obtained to the heat treatment when the powders were reused. The same heat treatments were applied to the 17-4 PH stainless steel obtained by the conventional method for comparison during evaluation. As a result of the preliminary studies, it has been seen that the solutionizing heat treatment (SHT) carried out at the temperature specified in the standard requires long periods to obtain a homogeneous microstructure of the additive manufacturing parts. It has been determined that the solutionizing heat treatment carried out for 1 hour at 1100°C provides a homogeneous microstructure. The heat treatments applied are given in Table 3.3 below.

Table 3.3 Heat treatment procedure

Heat Treatment Condition	*Temperature (°C)*	*Duration (h)*	*Cooling*
SHT	1100	1	Air Cool
H900	480	1	Air Cool
H1025	550	4	Air Cool
H1100	595	4	Air Cool

The furnace used for heat treatment is a Protherm brand specially produced furnace. It can go up to a maximum of 1300°C. Figure 3.16 shows the heat treatment furnace.

Figure 3.16. Heat treatment furnace

The samples were first solutionized at 1100°C followed by air cooling and then aging heat treatments were applied at 480°C, 550°C and 595°C in order to obtain the H900, H1025 and H1100 states respectively.

CHAPTER 4

RESULTS & DISCUSSION

In this part of the thesis, firstly the production process was explained and then the results of the tests performed on the powders and the final parts obtained as a result of additive production were shared. It has been tested how the properties of both the produced parts and the powders themselves have changed with the reuse of powders. The results were subjected to a comprehensive evaluation and explained in detail.

4.1 Production Details

17-4 PH stainless steel powders were used in the productions. Production has started with powders that have not been used before. The maximum amount of powder allowed by the powder chamber of the RBV unit of the equipment was fed into the equipment. A total of 10 productions were planned and the powder mass decrease followed during the productions and the maximum height of each production are summarized in the Table 4.1. Since no new powder was added during the productions and the same powders were used repeatedly, the amount of powder naturally decreased as the productions progressed. As the amount of powder decreased, the height of production was also reduced. The maximum height of each production was calculated in direct proportion, starting from the powder mass that entered the production.

Table 4.1 Summary of productions

Number of Production	*Initial powder mass (g)*	*Produced part*	*Production height (mm)*
1	2972,8	3 Tensile Test Specimen, Full Height Block	54
2	2315,3	Support Structure	45,5
3	2297,9	Support Structure	45,1
4	2132,3	Support Structure	41
5	1917,3	3 Tensile Test Specimen, Full Height Block	35,8
6	1724,0	Support Structure	32,2
7	1494,6	Support Structure	27,1
8	1289,4	Support Structure	22,4
9	1066,4	Support Structure	19,5
10	945,2	3 Tensile Test Specimen, Full Height Block	14

The parts obtained before and after they were removed from the equipment can be seen in Figure 4.1 and Figure 4.2.

a

b

c

d

e f g

Figure 4.1. Images taken during 1st, 5th and 10th productions (a,b), powder cleaning of the parts at the end of process (c,d) and produced final parts from the 1st (e), 5th (f) and 10th (g) productions

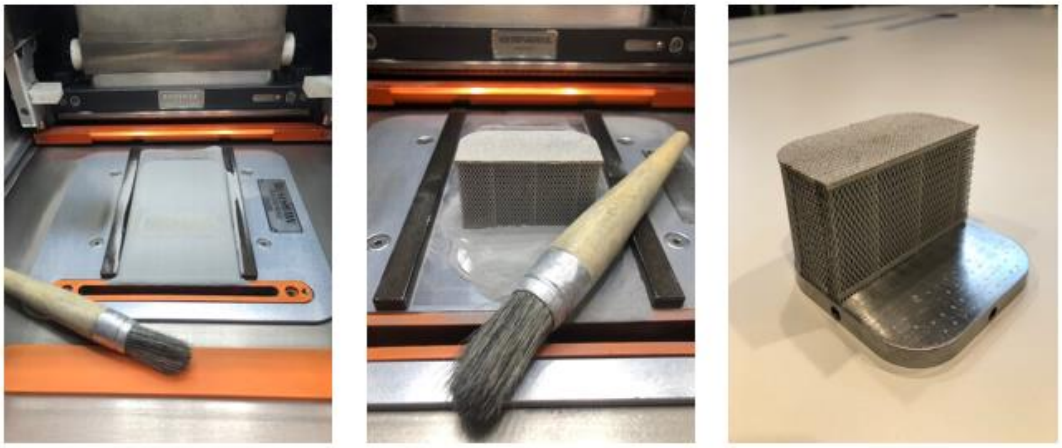

a b c

Figure 4.2. Image taken during intermediate productions (a), powder cleaning of the part at the end of process (b) and produced final part from the intermediate productions (c)

4.1.1 Filling Parts

Since it is planned to continue the productions without adding any new powder, the amount of powder will decrease in each new production. In the RBV unit, the volume of the powder bin is fixed. According to the SLM principle, the powder chamber rises as much as the layer thickness and this amount of powder is laid on the production table. In the case of this study, the powders are reduced after each production. In this case, the powder remaining in the productions after the first production will never be able to completely fill the powder chamber. For this reason, in every new production, the lower part of the powder chamber must be filled in order for the remaining powder to reach the upper surface of the chamber. It has been decided to place filling parts at the bottom of the powder container in order to fill the volume as much as the powder that is reduced in the powder container. For this purpose, a billet suitable for powder chamber dimensions was machined from Aluminum 6061 material. Slices were cut from this log according to the decreasing amount of powder at the beginning of each production and placed in the lower part of the chamber. Then the powders were placed on this part and the powders were allowed to reach the top of the chamber.

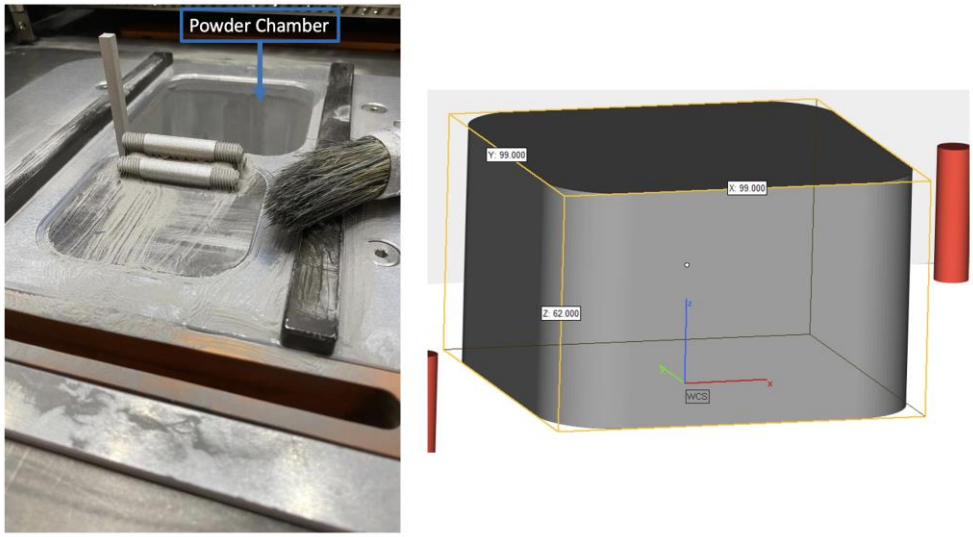

Figure 4.3. Powder chamber and its dimensions

4.2 Characterization Tests of 17-4 PH Stainless Steel Powders

Various characterization tests were applied to 17-4 PH stainless steel powders. The unused powders were tested at the first stage and then samples were taken from the powders at the end of 10^{th} production in order to see the changes in the powders as they were reused, following the appropriate sampling standards and subjected to tests.

4.2.1 Powder Morphology

While powder particles are considered completely spherical, the real situation is different. There are often defects on the surface of the particles. These errors affect how closely the powder particles can be packed together. Irregular particles are packed less densely than regular particles. Since the surface area of small powder particles is larger, they absorb the energy from the laser more efficiently during the process and are more prone to melting. Large particles of powder are less prone to complete melting. Metal powders undergo two types of shape deformation. These are satelliteization and agglomeration. Partial melting occurs when two-thirds of the melting temperature of the metal is reached. This is the mechanism of deformation formation. The sticking of small pieces to large ones during heating is called satelleization. The large particle usually remains spherical in an unmelted state. Agglomerated particles are formed when two or more partially molten powder particles come together. After this stage, this powder particle is deformed and there is no longer any talk of sphericity. Such deformations in the shapes affect the powder behavior. Packing of powders is affected, which in turn affects the density of the powder bed [50]. SEM was used to examine the shapes of the powders. SEM images of powders at different production levels are shown Figure 4.4 to Figure 4.12 below.

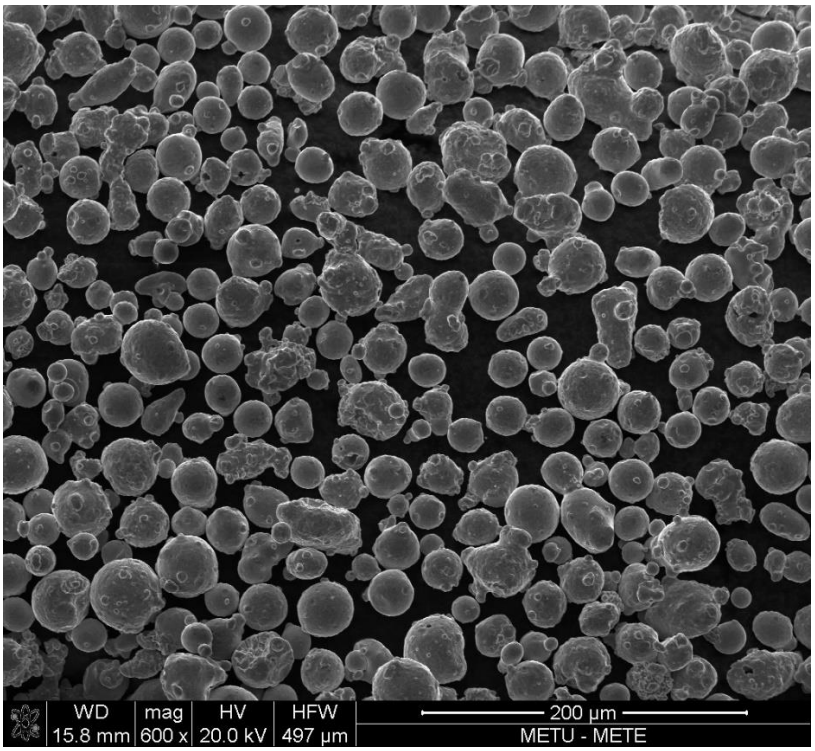

Figure 4.4. SEM images of unused 17-4 PH SS with 600x magnification

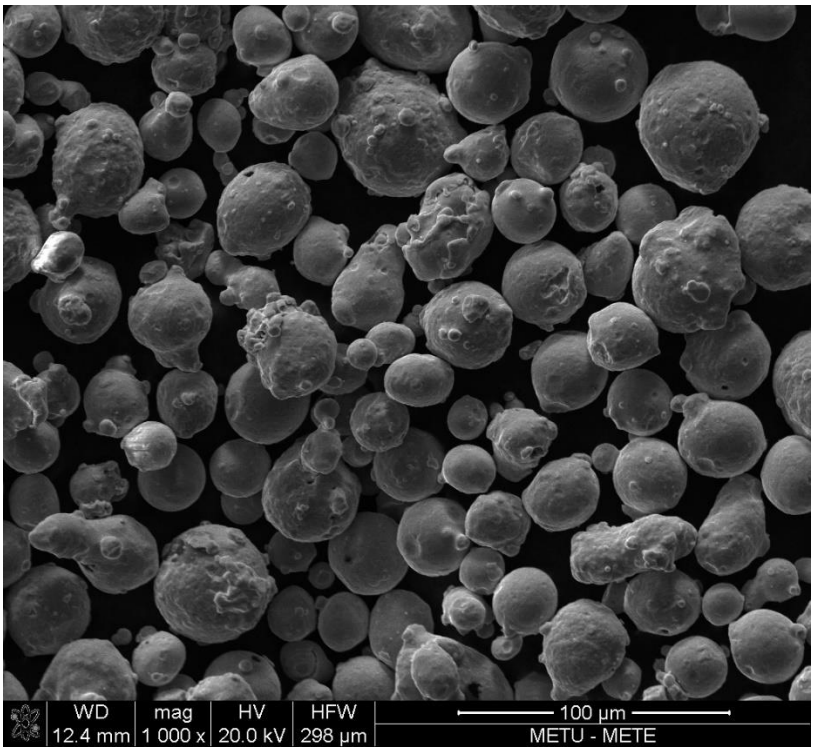

Figure 4.5. SEM images of unused 17-4 PH SS with 1000x magnification

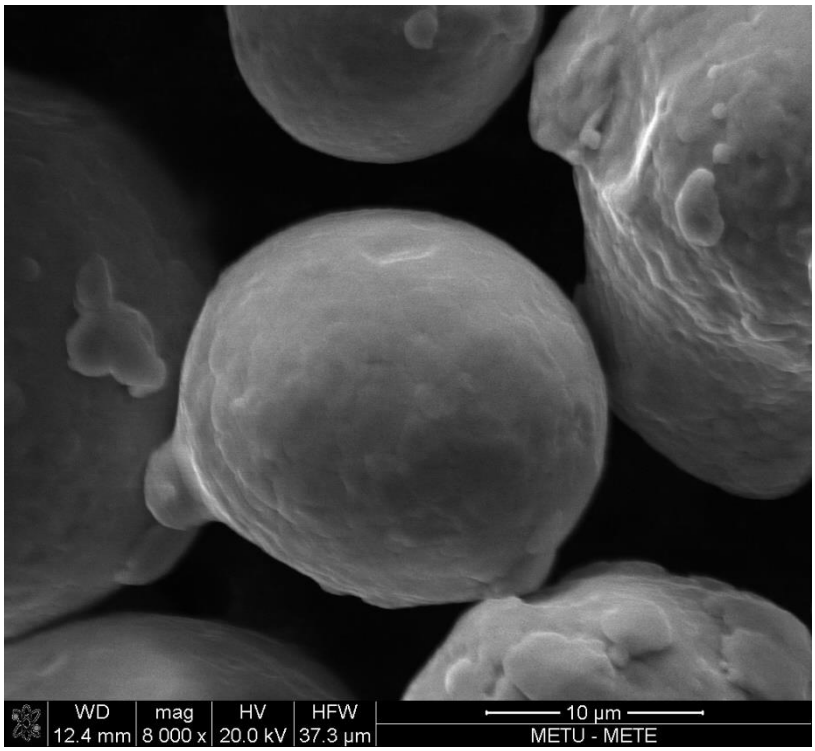

Figure 4.6. SEM images of unused 17-4 PH SS with 8000x magnification

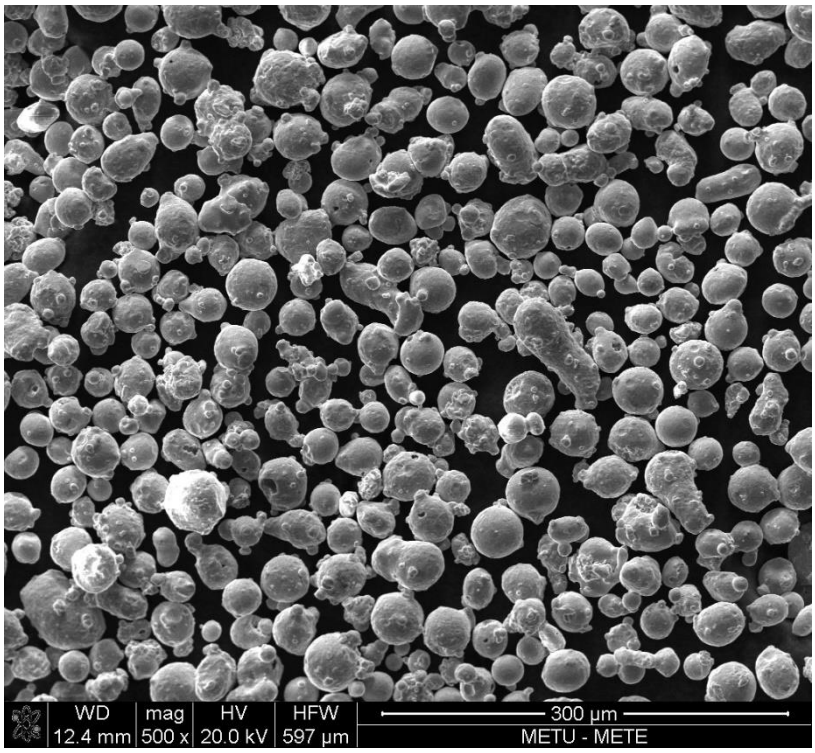

Figure 4.7. SEM images of 5 times used 17-4 PH SS with 500x magnification

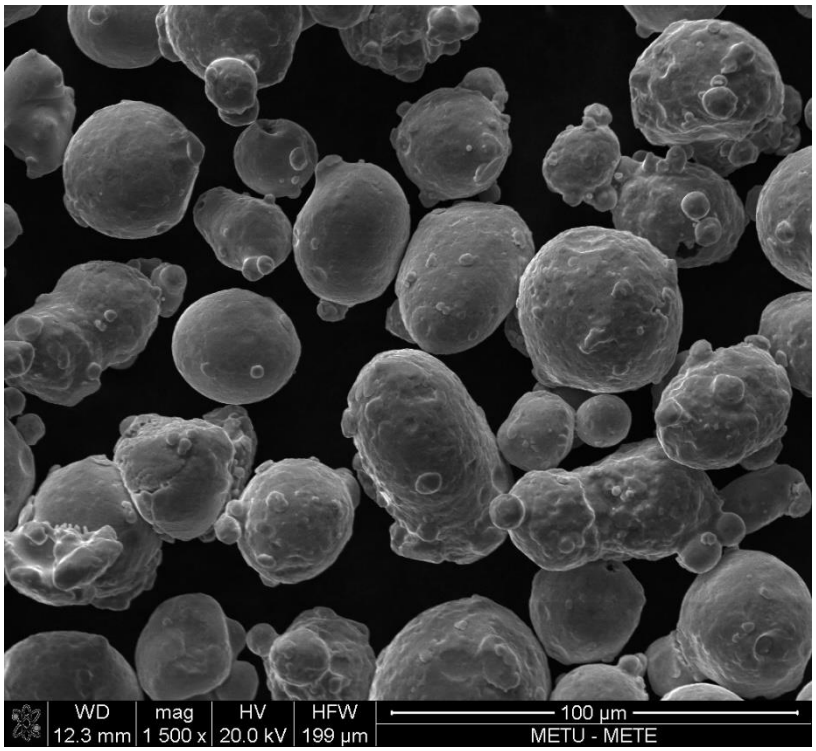

Figure 4.8. SEM images of 5 times used 17-4 PH SS with 1500x magnification

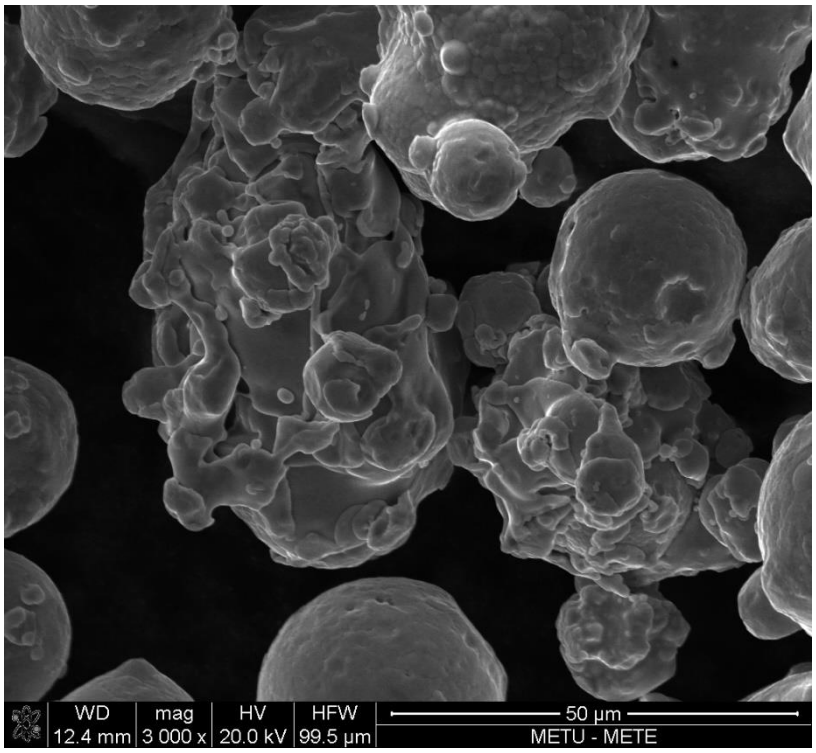

Figure 4.9. SEM images of 5 times used 17-4 PH SS with 3000x magnification

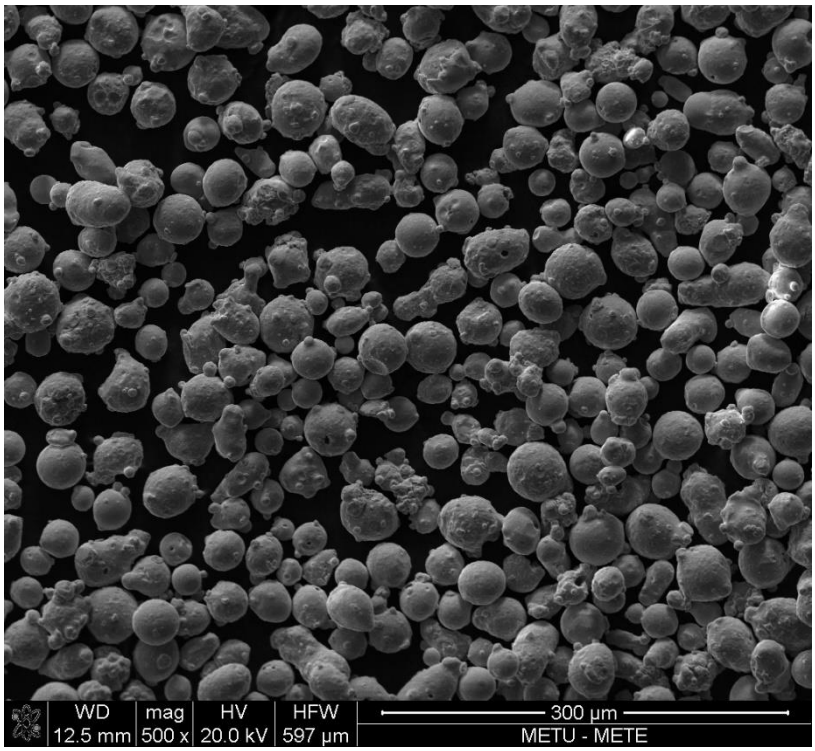

Figure 4.10. SEM images of 10 times used 17-4 PH SS with 500x magnification

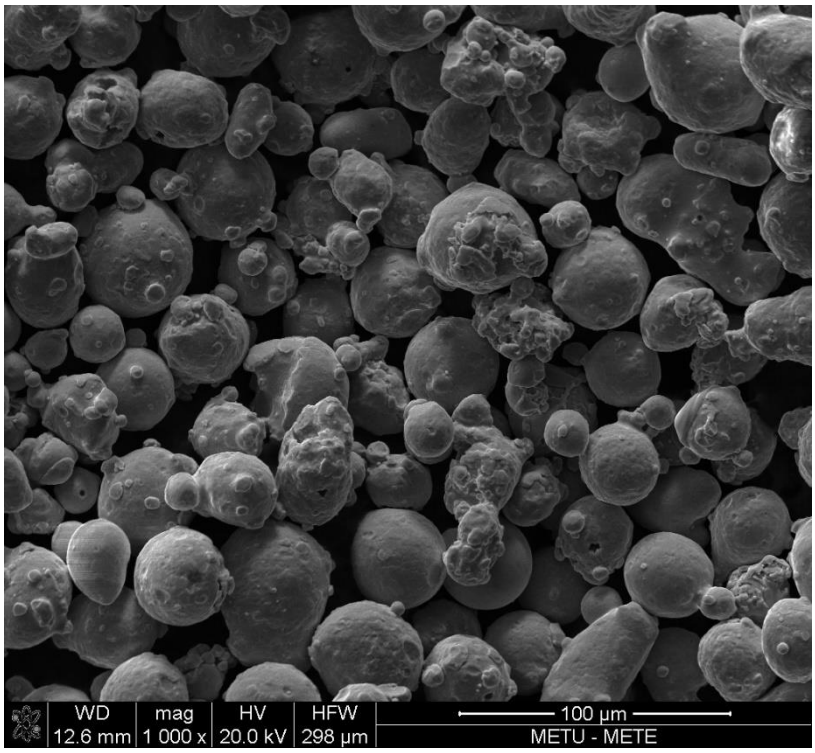

Figure 4.11. SEM images of 10 times used 17-4 PH SS with 1000x magnification

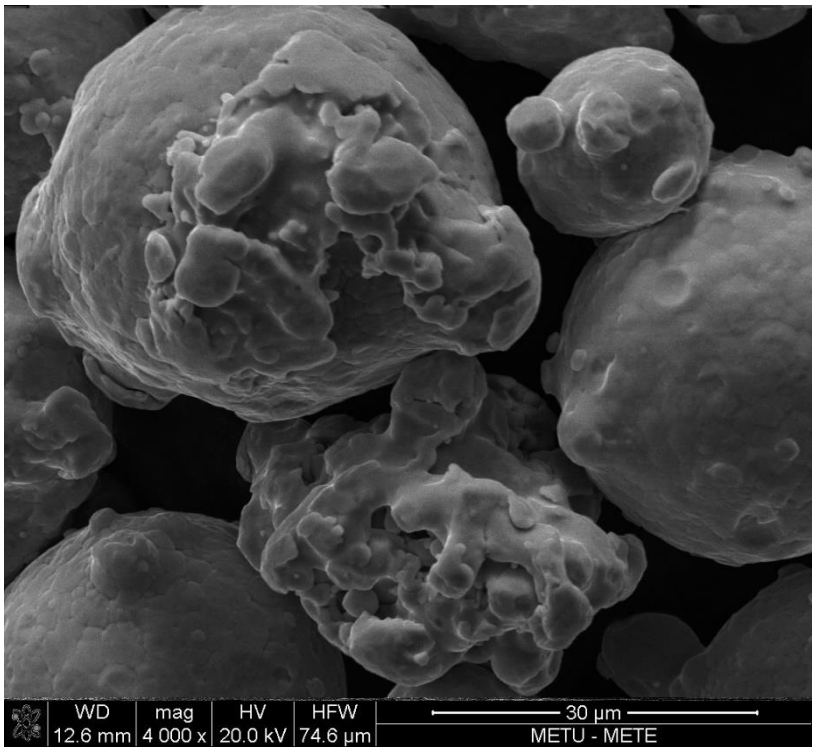

Figure 4.12. SEM images of 10 times used 17-4 PH SS with 4000x magnification

As can be seen from the SEM images, irregularly shaped powder particles are seen in the powders that have not yet entered production, that is, unused. However, when the overall powder sample is examined, the powders generally have a spherical shape. Small powder particles clinging to large powder particles are also seen. As mentioned before, this situation is called satellite formation. Since it is known that these powders were produced by the atomization process, it is thought that these are method related errors. When the images of the powder used 5 times were examined, it was seen that the powders with deformities slightly increased. There was also a minor increase in the formation of satellites. The shape distortions continued in the SEM images of the powders that were used 10 times. It is useful to underline that these powder samples were prepared after sieving with a 45 microns sieve. Therefore, it was expected that no abnormally large powder particles should be encountered.

4.2.2 Powder Density Measurements

The true density, bulk density and tapped density of the powders were measured and the results were evaluated in the subheadings of this section.

4.2.2.1 True Density Measurements

As explained under the heading 3.4.3.1, the actual density values were measured by the helium pycnometry method. It is considered that the true density value corresponds to the density of the part produced at 100% occupancy. If the powders have a porous structure and these pores are on the surface, the actual metal density can still be determined by this method, but if there are hollow powder particles, helium gas cannot reach these spaces and these spaces are calculated as a part of the powder. In such a case, the measured true density value of the powder may be slightly lower than the density of the metal part produced [22]. The measured true density values of the unused powder at the beginning of the productions and the 10 times used powder removed from the last production are given in Table 4.2.

Table 4.2 Densities of powders in g/cm^3

Number of Measurement	*Unused powder*	*10 times used powder*
1	7.5675	7.6139
2	7.5778	7.6202
3	7.5659	7.6166
Average	7.5704	7.6169
Standard Deviation	0.0065	0.0032
Confidence Interval (95%)	0.0073	0.0036

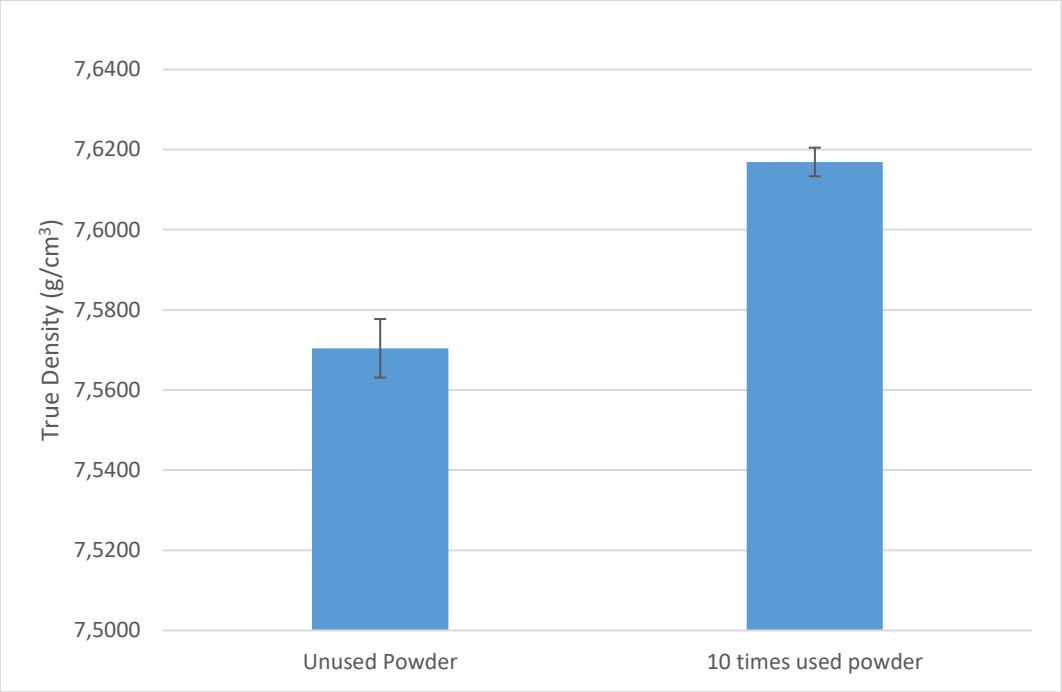

Figure 4.13. True density graph

When the density value of the part obtained as a result of the 1st production given under the heading 4.3.1, measured by the Archimedes method, and the true density of the unused powder were compared, it is seen that the part density was obtained at higher value. However, the density of the part obtained in the final production has almost the same value as the true powder density measured for the 10 times used powder. Based on the literature, it can be interpreted that there may be intra-powder porosity in the starting powders and that the amount of powders with hollows decreases as a result of the reuse of the powder. For this reason, the true powder density measured and the density of the obtained part gave almost the same result in the 10th use.

4.2.2.2 Bulk and Tapped Density Measurements

Bulk density (also called apparent density) is the density measured as the powder settles only with the effect of gravity. No other force acts on the powders. Bulk density values measured using Hall flowmeter are given in Table 4.3 below. The density measured when the powder bed is tapped is the tapped density value. This feature often simulates the situation where powders are closely packed [51]. Tapped density measurement results are given in Table 4.4. Bulk density and tapped density are used in the interpretation of the powder flow. This is explained in more detail in chapter 4.2.5.

Table 4.3 Bulk densities of powders in g/cm^3

Number of Measurement	*Unused powder*	*10 times used powder*
1	4.10	3.92
2	4.05	3.93
3	4.05	3.97
Average	4.07	3.94
Standard Deviation	0.03	0.03
Confidence Interval (95%)	0.03	0.03

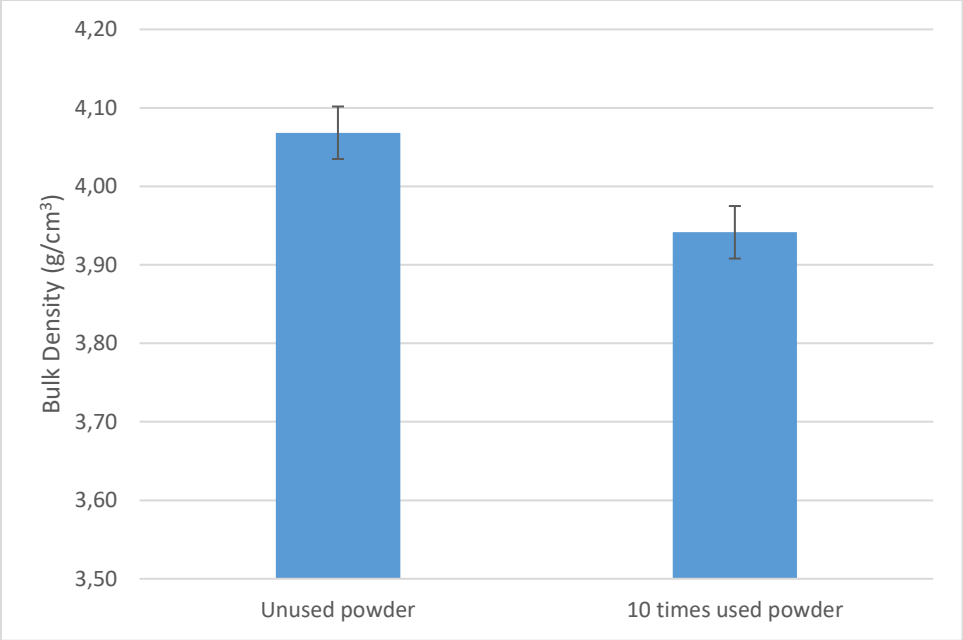

Figure 4.14. Bulk density graph

As seen in Figure 4.14, as the powders were reused, the bulk density decreased.

Table 4.4 Tapped densities of powders in g/cm^3

Number of Measurement	*Unused powder*	*10 times used powder*
1	4.56	4.52
2	4.51	4.57
3	4.45	4.54
Average	4.51	4.54
Standard Deviation	0.05	0.03
Confidence Interval (95%)	0.06	0.03

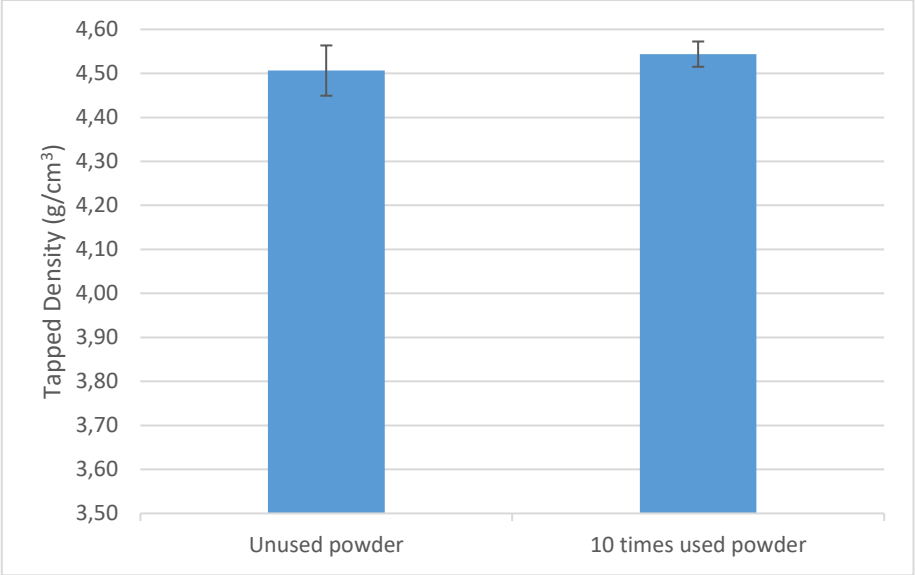

Figure 4.15. Tapped density graph

It was found that the tapped density value remained unchanged as the powders were reused. In the literature, it has been written that more dense parts are obtained from the production made with powders with a high tapped density [52]. In the results obtained in this thesis, no significant difference was measured between the first production and the 10^{th} production in terms of density. The fact that there is no difference in the tapped density values and the densities of the final parts are close support each other.

4.2.3 Particle Size Distribution of Powders

Dynamic image analysis is the method by which information about the particle size distribution and shapes of the powders is obtained. During this test, approximately 10 million particles were monitored with high resolution cameras to obtain information about particle size distribution and shape.

Figure 4.16. Powder image monitored by CamsizerX2 equipment

The results obtained when tested with dynamic image analysis were summarized in Table 4.5 below.

Table 4.5 Particle size distribution of powders

Number of Recycle	*D10*	*D50*	*D90*
0	22.54	31.51	41.71
10	22.11	30.91	41.01

Percentages are indicated by the letter D followed by the % value. So, D10=22.54 μm, D50=31.51 μm and D90=41.71 μm means that 10% of the sample is less than 22.54 μm, 50% less than 31.51 μm and 90% less than 41.71 μm. Particle size distribution graphs of unused powder and 10 times used powder were given in the figure below. Since the powders were sieved with a 45 μm before each production, very high dimensional particles are not expected in the results. The tiny peak seen around 80 μm in the graph of the powder used 10 times may have been caused by

the device processing another contaminated particle. As can be seen, almost no change was obtained in the particle size distribution.

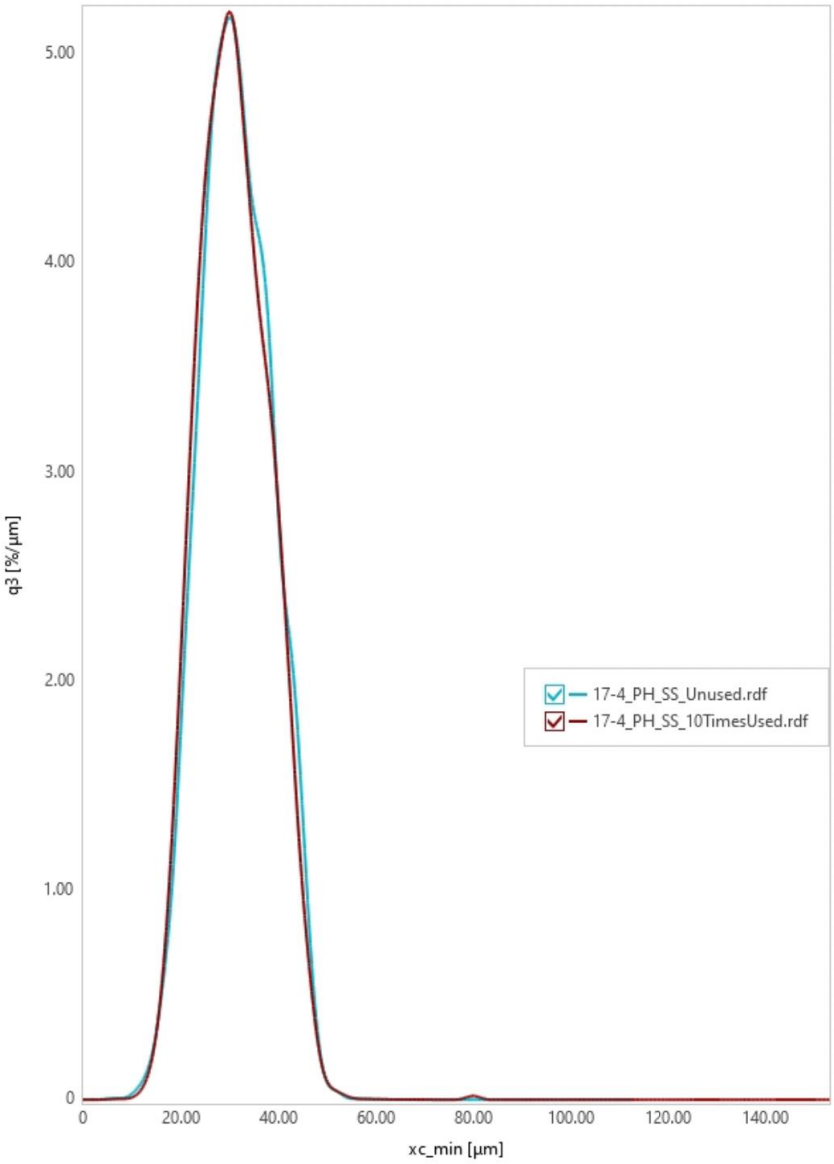

Figure 4.17. Particle size distribution curves

Spherical particles are more preferable than deformed particles because they give better packing density. The measure of how round a powder particle is its aspect ratio. The aspect ratio (width/length) is measured on a scale of 0 to 1, with elongated shapes having lower values and indicating that the particle is not spherical.

Therefore, aspect ratio is a common parameter to check when measuring whether a powder is suitable for an additive manufacturing process. While the average aspect ratio of unused powders was 0.81, the average aspect ratio of the powders used 10 times was obtained 0.82. As can be seen, there is not much difference in the aspect ratios but it can be interpreted that the shapes of the powders get a little closer to spherical as they are used.

4.2.4 Chemical Composition of Powders

The chemical composition of the powder fed to additive manufacturing is one of the important features to be considered when deciding whether the final piece produced will be suitable for use in the planned application area. For the chemical composition of the powders to change, it must first undergo a chemical reaction. The presence of agents that can react with powders such as oxygen, nitrogen, carbon in the air causes chemical reactions. In the metal additive manufacturing process, this is of minor importance because inert gas is supplied to the production area. However, this does not prevent all contamination. There are other situations that can cause a reaction at the time of manufacture. Even if production under inert gas reduces the possibility of chemical reaction, there are two situations that will increase the desire of metal powders to enter chemical reactions. These are surface area and temperature. In additive manufacturing, powders have a large surface area. That is, the area available for reaction is quite large. Although the presence of an inert gas somewhat compensates for this situation, the real possibility of reaction occurs when the powders are transported without an inert gas environment. Many reactive gas molecules can interact with the powders because there is no inert gas environment when the powders are removed from the production equipment and the sieving process is carried out. As time passes, the chemical composition of powder particles changes. Keeping the production area at a high temperature during production also increases the possibility of powder reaction. However, this is less likely as preheating is not usually applied in the SLM process [50].

Table 4.6 Chemical composition of powders in wt% before and after productions

Element	*Carpenter Data Sheet*	*Unused Powder*	*10 times used powder*
Nickel (Ni)	3.00-5.00	4.225	4.388
Niobium (Nb)	0.15-0.45 (Nb+Ta)	0.270	0.286
Tantalum (Ta)	0.15-0.45 (Nb+Ta)	0.028	0.028
Chromium (Cr)	15.00-17.50	16.76	16.646
Silicon (Si)	1.00 max	0.466	0.522
Copper (Cu)	3.00-5.00	4.331	4.402
Manganese (Mn)	1.00 max	0.221	0.222
Iron (Fe)	rest	rest	rest

There is no tangible change in the chemical composition of the powders. The oxygen, nitrogen, carbon and sulfur contents of the powders are also examined (Table 4.7).

Table 4.7 Oxygen, Nitrogen, Carbon and Sulphur content of powders in ppm

Element	*Unused Powder*	*10 times used powder*
Oxygen	488.6	567.4
Nitrogen	290.4	339.5
Carbon	153.0	168.0
Sulphur	33.0	36.0

As it can be seen from Table 4.7, the oxygen, nitrogen, carbon and sulphur amount of the powders increased. The powders have been contaminated since the inert gas environment is not provided during the transport and sieving steps away from the production area. Considering the value range of these elements in the 17-4 PH stainless steel powder material specification (see table 3.1), the values remain within the determined limits. However, it is seen that as the powders continue to be used more, the powder material will go out of specification and cause a decrease in material properties due to this contamination.

4.2.5 Flow Properties

The flow rate of the powders was measured with a Hall flowmeter. The results obtained were given in Table 4.8 below.

Table 4.8 Flow rates of powders in s/50gr before and after productions

Number of Measurement	*Unused powder*	*10 times used powder*
1	21.0	30.0
2	22.0	31.0
3	22.0	29.0
Average	21.7	30.0
Standard Deviation	0.6	1.0
Confidence Interval (95%)	0.7	1.1

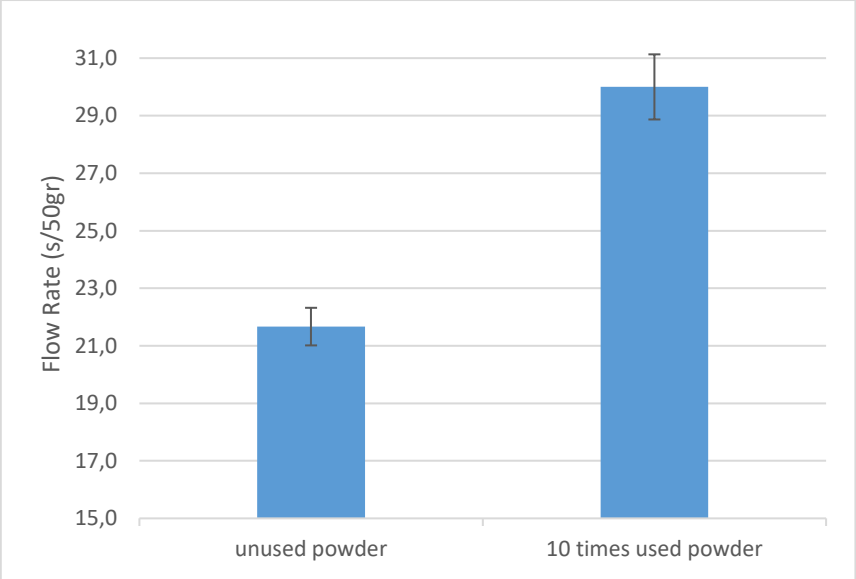

Figure 4.18. Flow rate graph

It has been observed that the powders flow slower as they are reused. Considering the satellization and agglomerations that occur in the shape of the powders as they are used, it is interpreted that there is deterioration in the flow properties due to the increase in friction between the powder particles compared to the initial situation. Another data used to comment on powder flow properties is the Hausner ratio. The hausner ratio is a value found by dividing the tapped density by the bulk density. If the Hausner ratio is higher than 1.25, the powder fluidity is classified as weak [53]. Calculated Hausner ratio values are shown in Table 4.9 below. Looking at the results, the Hausner ratio of the powder used 10 times was higher than the unused powder. However, it is still within the range of values showing good flow properties.

Table 4.9 Hausner ratio calculations

Powder Condition	*Bulk Density (g/cm^3)*	*Tapped Density (g/cm^3)*	*Hausner Ratio*
Unused	4.07	4.51	1.11
10 times used	3.94	4.54	1.15

4.3 Characterization Tests of 17-4 PH Stainless Steel Final Parts

Various characterization tests were applied to 17-4 PH stainless steel final parts produced via SLM process. The mechanical properties were determined by applying the tensile test to the tensile test specimens produced in the 1st, 5th and 10th productions. Characterization processes were applied by creating samples from the block piece produced.

4.3.1 Density Measurements of Final Parts

The densities of the produced parts were measured with the Archimedes principle. The results are given in Table 4.10 below.

Table 4.10 Density of final parts in g/cm^3

Number of Measurement	*Production 1*	*Production 5*	*Production 10*
1	7.639	7.624	7.618
2	7.640	7.622	7.614
3	7.638	7.626	7.621
Average	7.639	7.624	7.618
Standard Deviation	0.001	0.002	0.004
Confidence Interval (95%)	0.001	0.002	0.004

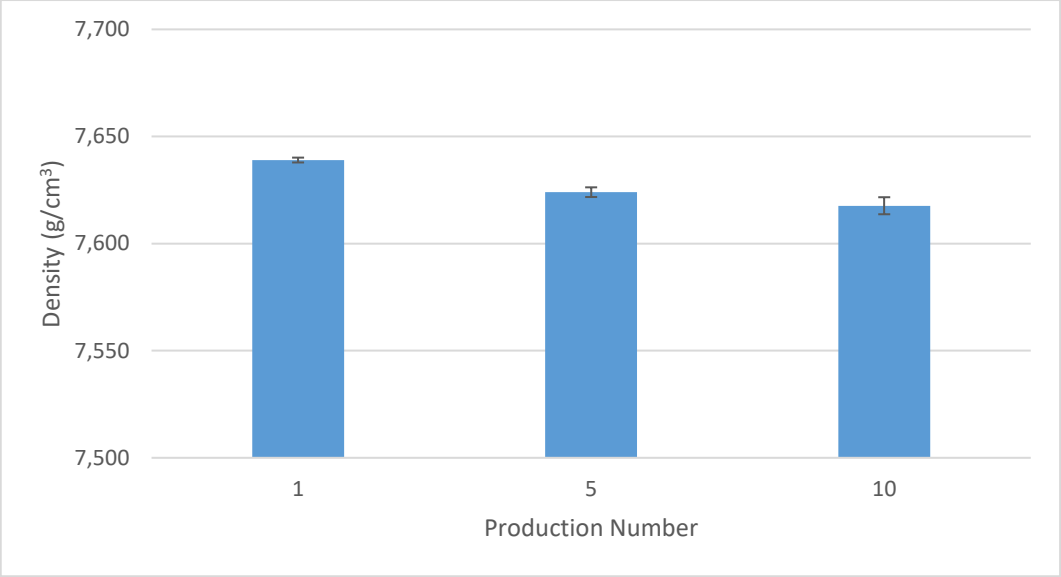

Figure 4.19. Archimedes density result graph

In the first production with unused powders, the highest density of parts was obtained. There is almost no difference between the densities of the pieces obtained from the 5th and 10th production.

4.3.2 Optical Occupancy Analysis of Final Parts

The optical occupancy rate was examined with the program called ImageJ using the images taken from the polished surfaces of the parts with an optical microscope. 3 images from each piece were examined and then averaged.

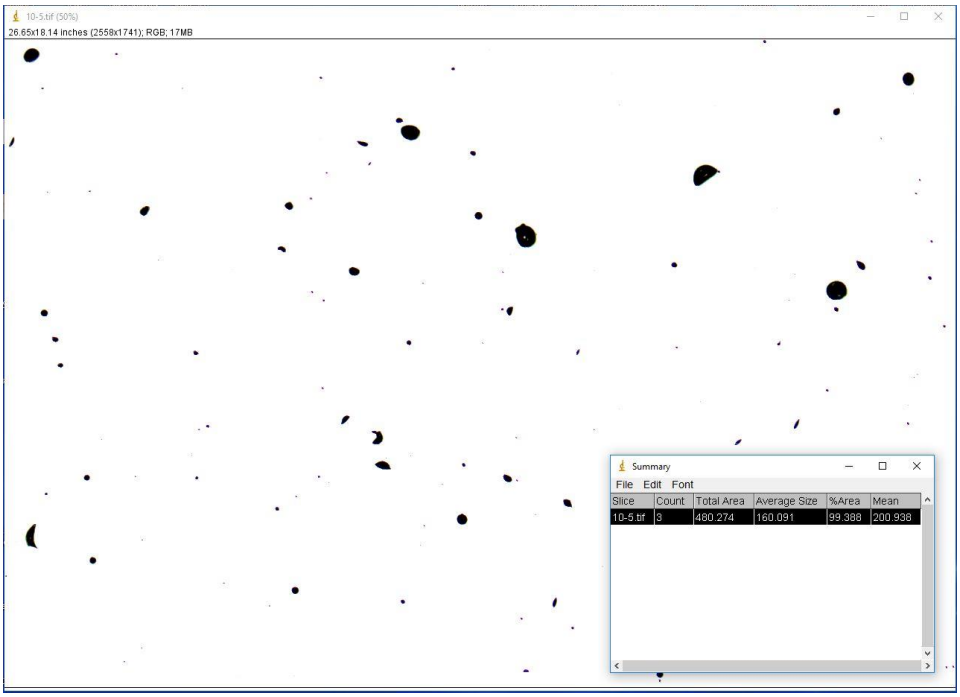

Figure 4.20. ImageJ program's result screen

It would be correct to interprete the percent occupancy results together with Archimedes density measurements. While determining the occupancy, a theoretical value is not used, the percent occupancy rate is obtained by determining the porosities in the material completely. However, a theoretical value is required to calculate Archimedes results as percent relative density. As a result of the laser hitting each layer in the SLM process, it somehow creates an aging effect on the previous layers [20]. For this reason, the density value of H900 heat treated 17-4 PH stainless steel produced by the conventional method was used as the theoretical maximum in the relative density calculations. This value was found to be 7.741 g/cm^3 as a result of the measurements made and the necessary calculations were carried out.

Table 4.11 Density and occupancy results

Production Number	*Density (Archimedes) (g/cm^3)*	*Archimedes' Method Relative Density (%)*	*Image Analysis Relative Density (%)*
1	7.639	98.682	99.419
5	7.624	98.489	99.309
10	7.618	98.411	99.290

It has been observed that there is a difference between the results obtained by the Archimedes method and the optical method. The reason for this can be explained as follows: 3 images, which are thought to represent the whole sample, were examined by optical method. It was interpreted that this method was insufficient to represent the whole sample. However, when looking at the trends, they showed similar behavior with each other. As the reuse of the powder increased, the density of the obtained product decreased slightly.

4.3.3 Chemical Composition Measurements of Final Parts

In order to measure the final parts' chemical composition, scanning electron microscopy (SEM) accompanied by energy dispersive elemental analysis (EDS) was used.

Table 4.12 Chemical compositions obtained via EDS analysis

Element	*Production 1*	*Production 5*	*Production 10*
Nickel (Ni)	4.18	4.99	4.99
Chromium (Cr)	16.99	16.46	16.71
Copper (Cu)	5.57	4.94	4.06
Manganese (Mn)	0.62	0.62	0.98
Iron (Fe)	72.64	72.99	73.26

When the chemical composition changes in the productions carried out with the reuse of powders were examined, it was seen that the biggest change was experienced in the copper element content. It had been determined that the copper ratio decreased gradually in the last piece as the powder was reused.

4.3.4 Surface Roughness Measurements of Final Parts

Surface roughness measurements were made on the block piece produced in the 1st, 5th and 10th productions. Since the area of the upper surface of block is very small (0.5x0.5 mm), measurements were taken from the side surfaces along the xy direction.

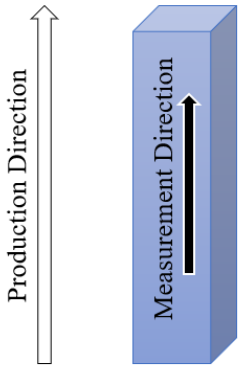

Figure 4.21. Surface roughness measurement direction

In order to increase reliability, measurements were taken four times from four surfaces. The results are given in Table 4.13 below.

Table 4.13 Surface roughness of final parts in μm

Number of Measurement	*Production 1*	*Production 5*	*Production 10*
1	5.83	7.78	5.85
2	6.46	6.31	5.32
3	5.67	7.79	5.85
4	6.50	5.58	5.72
Average	6.12	6.87	5.69
Standard Deviation	0.43	1.10	0.25
Confidence Interval (95%)	0.42	1.08	0.25

When the results were examined, it was seen that the surface roughness of the produced parts increased as the powders were reused until the 5^{th} production. However, it was observed that the surface roughness of the part that came out of the last production made with reused powders until the 10^{th} production was even lower than the first production made with unused powder. Considering the confidence intervals of the measurements, it can be interpreted that reuse of the powders 10 times does not have a significant effect on the surface roughness of the produced parts, since the values remain within the variances of each other.

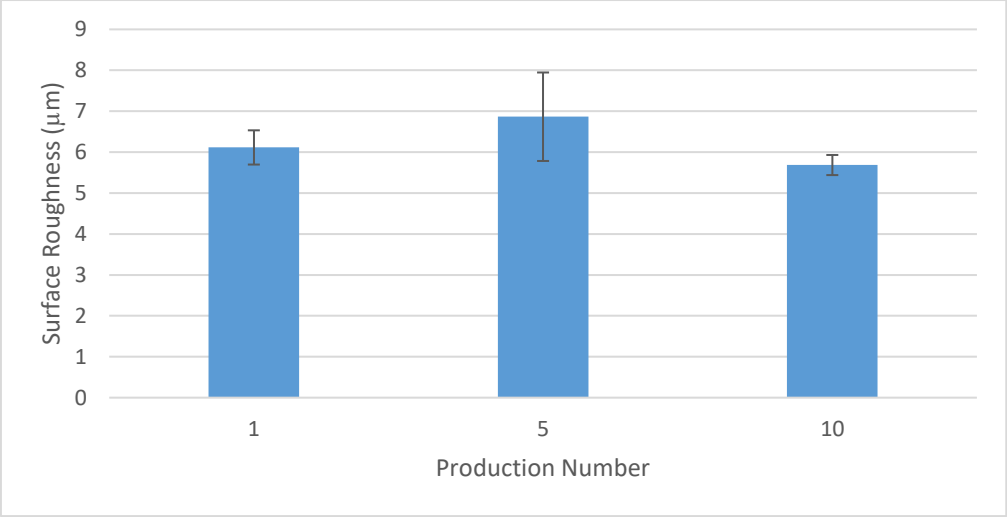

Figure 4.22. Surface roughness graph

4.3.5 Tensile Test Results of Final Parts

Tensile test was applied to the produced tensile test specimens in as-built condition. Elongation data were monitored. The results were given in Table 4.14, Table 4.15 and Table 4.16 below.

Table 4.14 Tensile test results of production 1

Specimen Number	*Yield Strength (MPa)*	*Ultimate Tensile Strength (MPa)*	*Elongation (%)*
1	871.00	931.00	14.20
2	889.00	940.00	17.80
3	880.00	971.00	14.70
Average	880.00	947.33	15.57
Standard Deviation	9.00	20.98	1.95
Confidence Interval (95%)	10.18	23.75	2.21

Table 4.15 Tensile test results of production 5

Specimen Number	*Yield Strength (MPa)*	*Ultimate Tensile Strength (MPa)*	*Elongation (%)*
1	842.00	914.00	17.10
2	886.00	966.00	15.80
3	845.00	902.00	17.50
Average	857.67	927.33	16.80
Standard Deviation	24.58	34.02	0.89
Confidence Interval (95%)	27.82	38.50	1.01

Table 4.16 Tensile test results of production 10

Specimen Number	*Yield Strength (MPa)*	*Ultimate Tensile Strength (MPa)*	*Elongation (%)*
1	888.00	949.00	19.30
2	863.00	933.00	11.30
3	874.00	928.00	11.30
Average	875.00	936.67	13.97
Standard Deviation	12.53	10.97	4.62
Confidence Interval (95%)	14.18	12.41	5.23

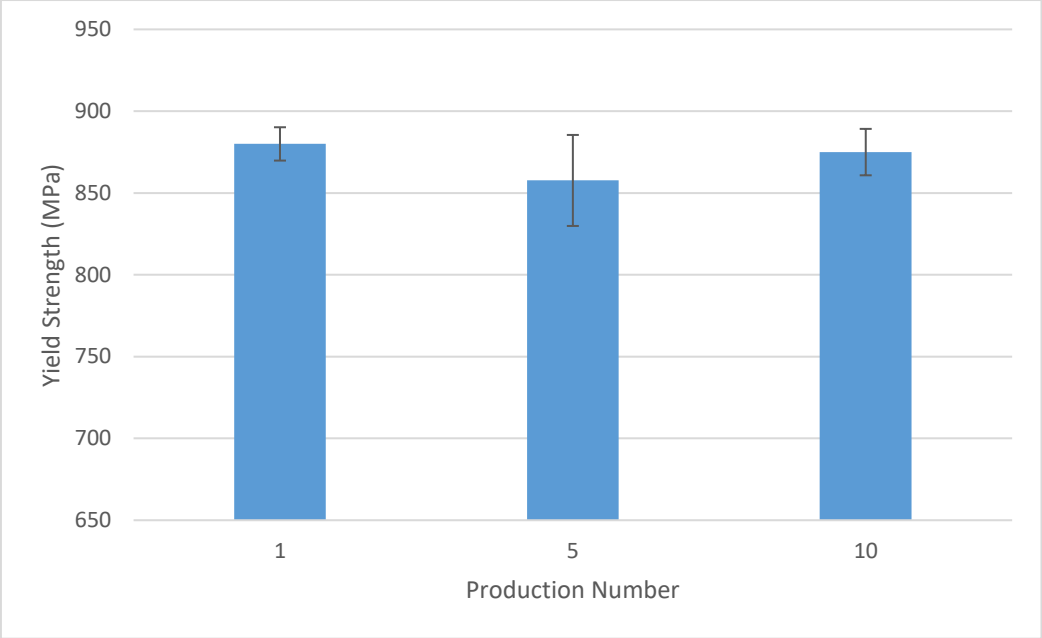

Figure 4.23. Yield strength comparison chart

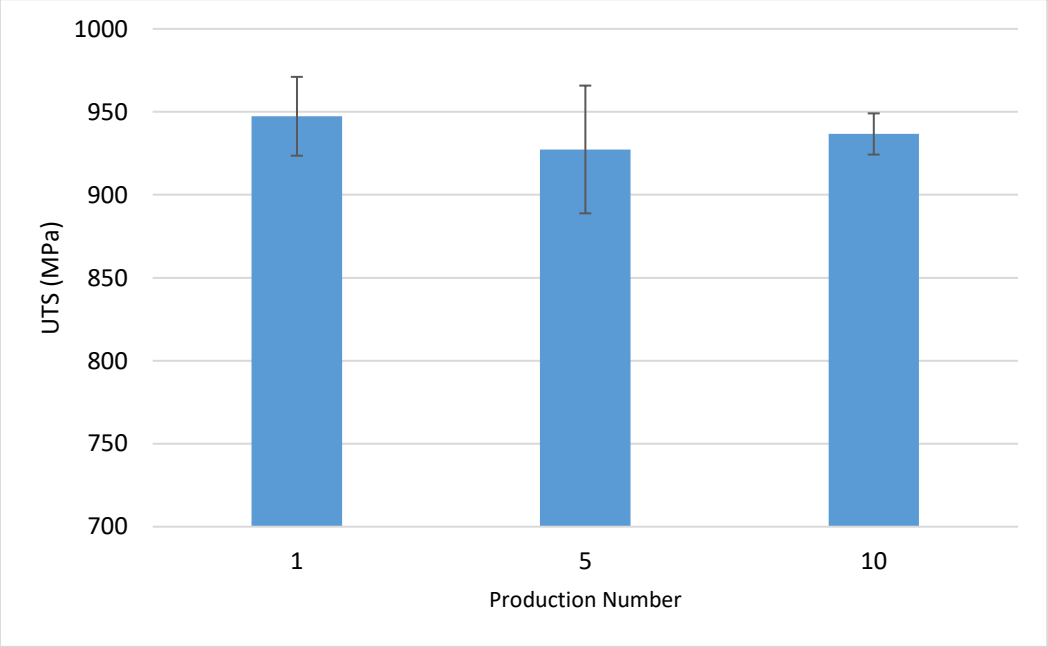

Figure 4.24. Ultimate tensile strength (UTS) comparison chart

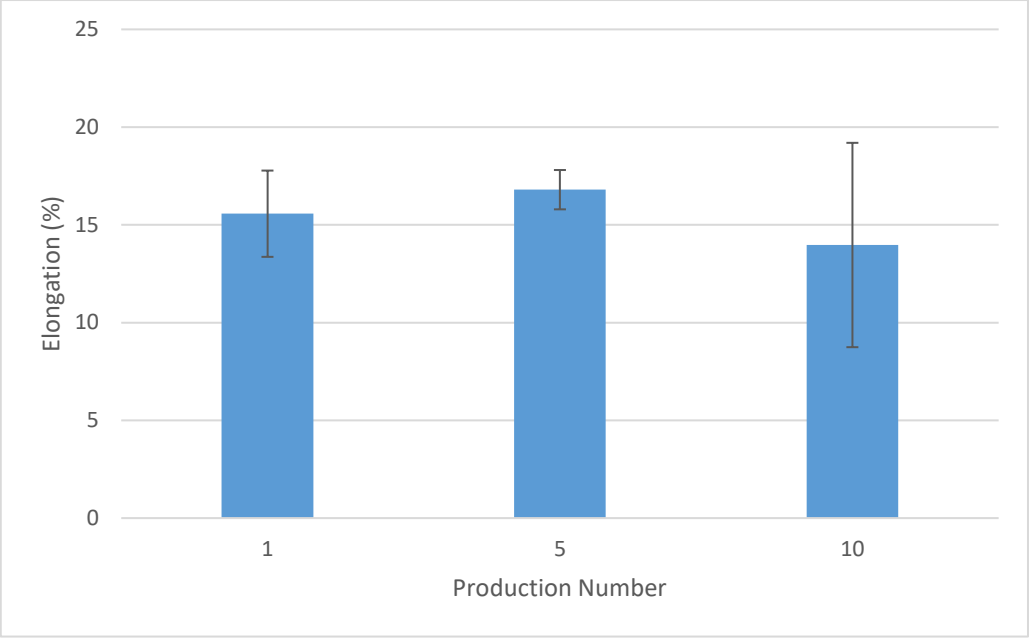

Figure 4.25. Elongation comparison chart

Since all values remained within the variance of each other, it was observed that the reuse of powders did not cause a significant change in the tensile properties for at least 10 productions.

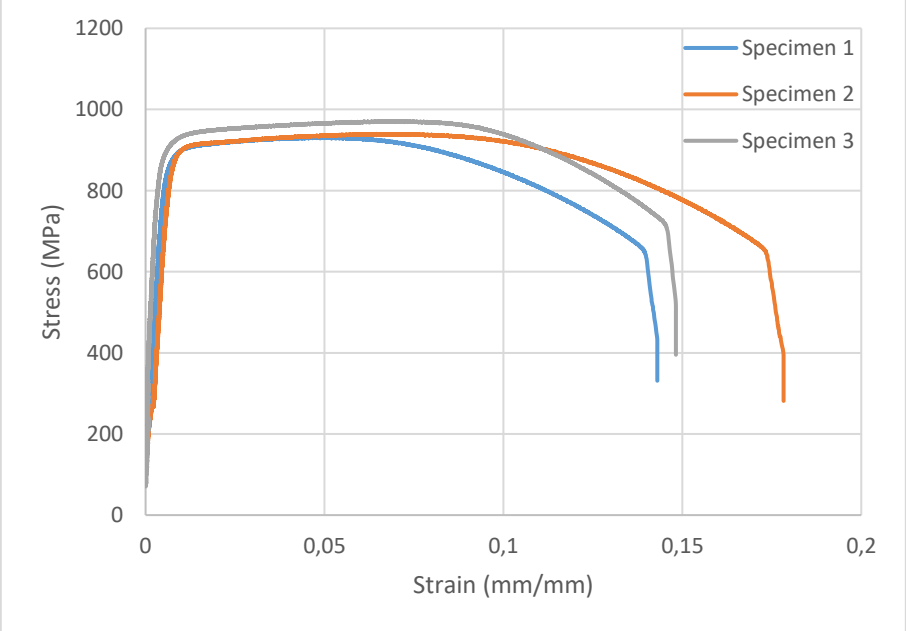

Figure 4.26. Production 1 stress-strain graph

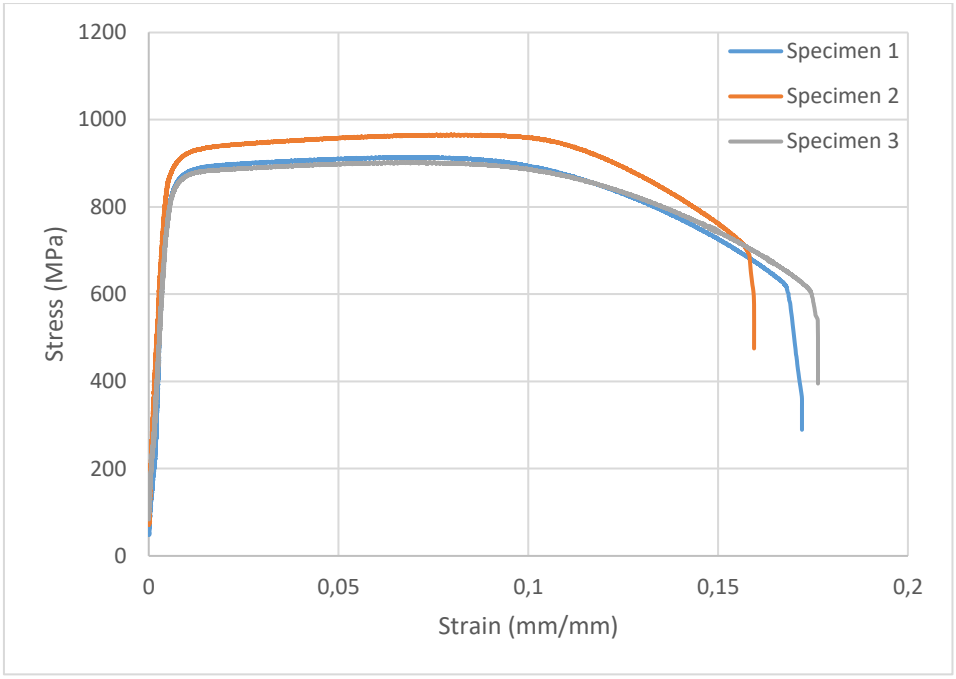

Figure 4.27. Production 5 stress-strain graph

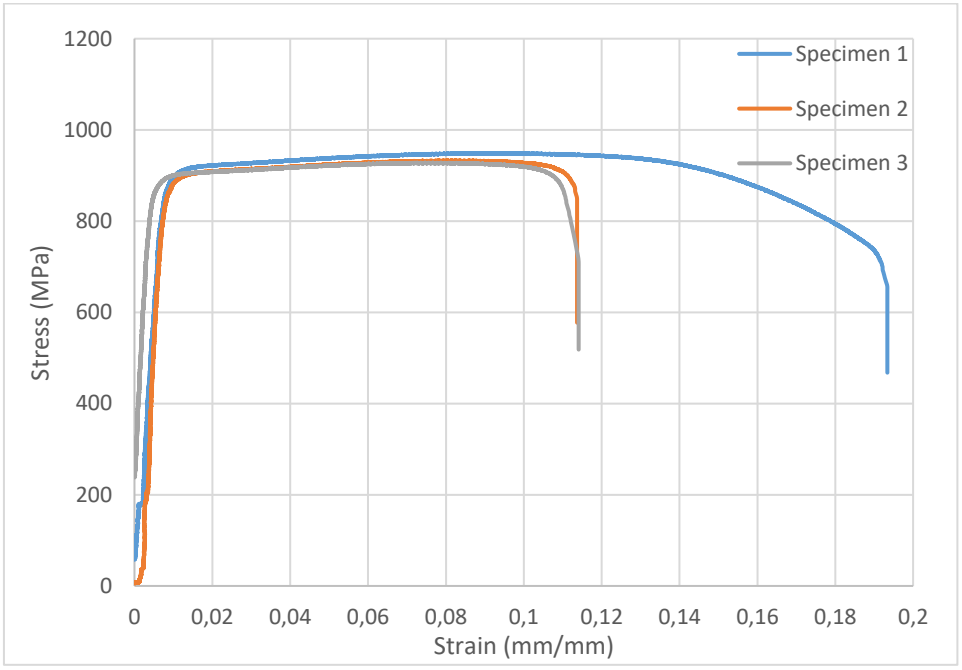

Figure 4.28. Production 10 stress-strain graph

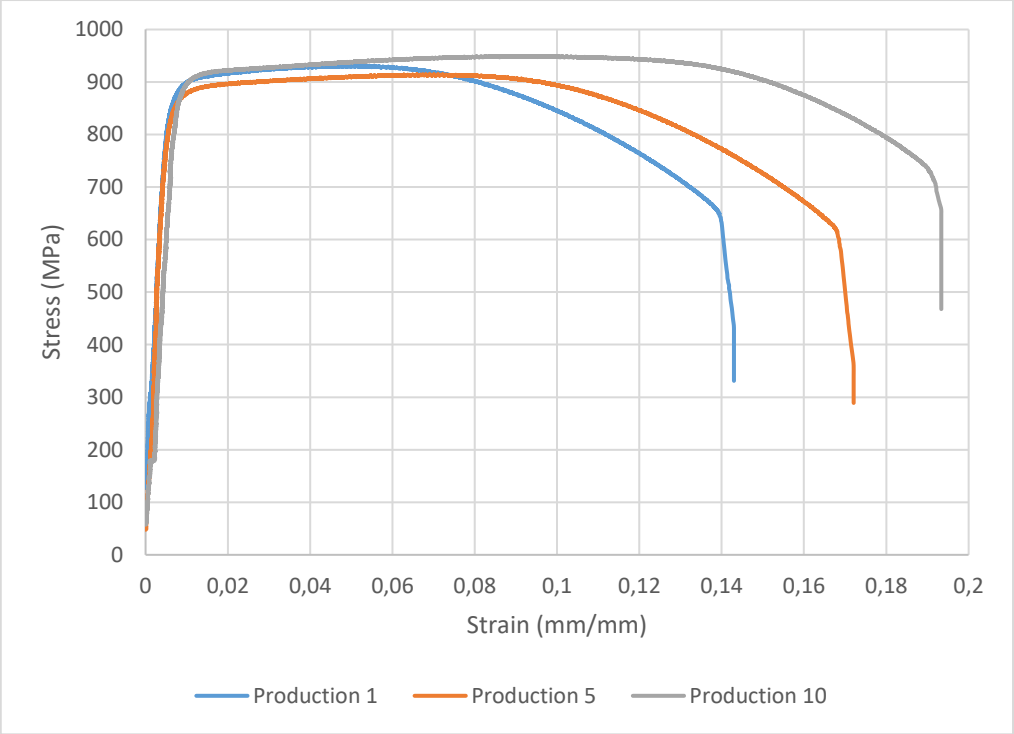

Figure 4.29. Comparison chart of the tensile test results of the parts obtained in the 1st, 5th and 10th productions

4.3.5.1 Fracture Surface Examination

After the tensile test, the fracture surfaces were examined under SEM. Since the fracture surfaces of specimens of the 1st and 5th productions were similar, images of one of each production were given to create an example. However, due to the elongation difference between specimen 1 and 3 in the 10th production, these specimens were handled separately. The obtained images are given from Figure 4.30 to Figure 4.33.

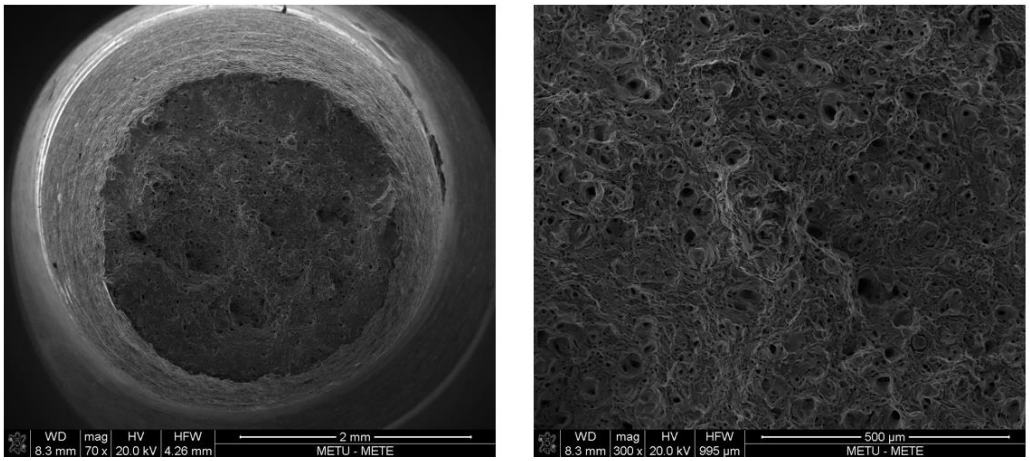

Figure 4.30. Fracture surface of specimens obtained from production 1

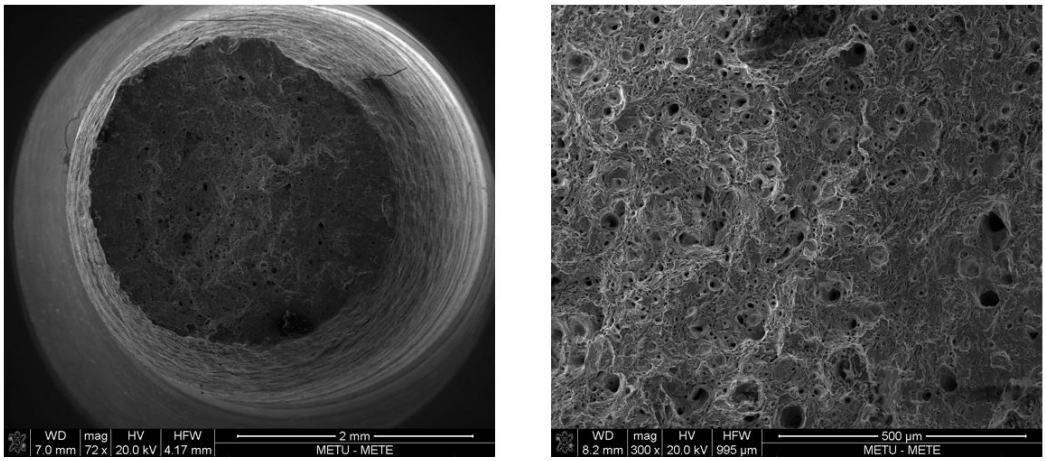

Figure 4.31. Fracture surface of specimens obtained from production 5

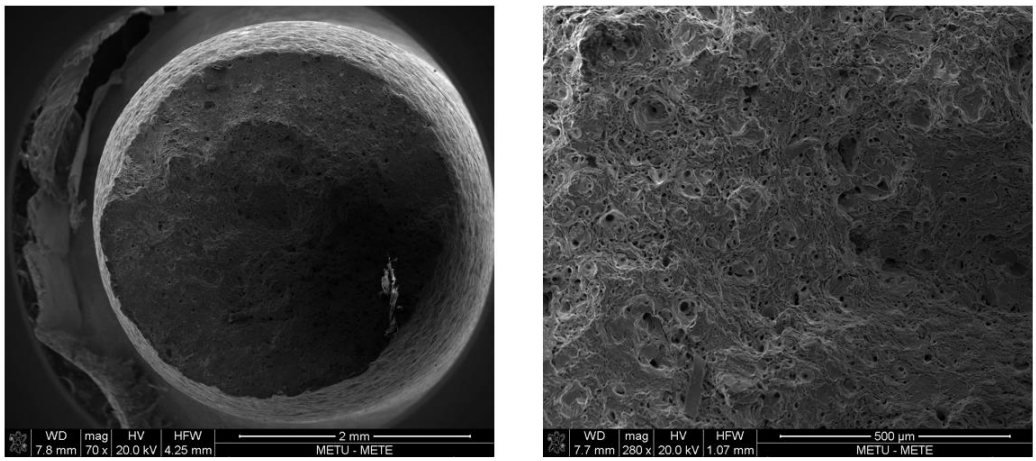

Figure 4.32. Fracture surface of specimen 3 obtained from production 10

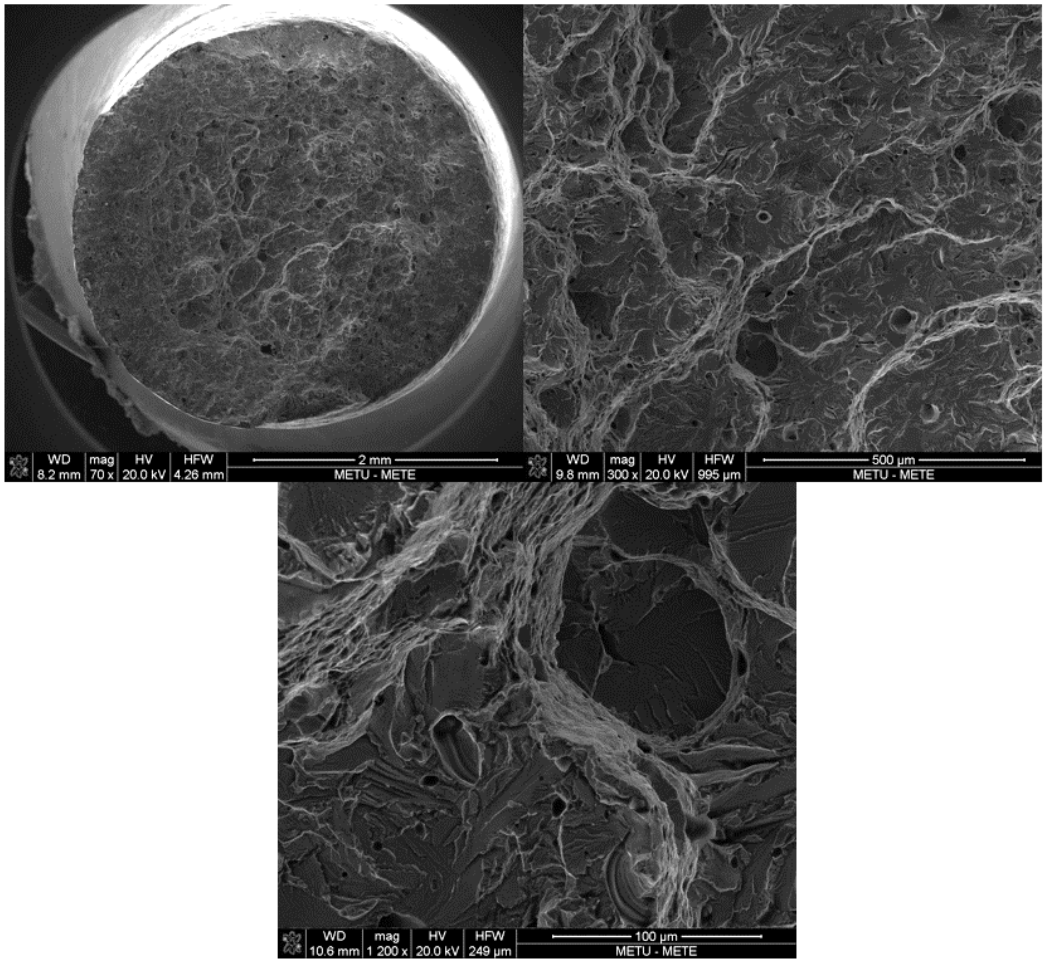

Figure 4.33. Fracture surface of specimen 1 obtained from production 10

While dimples indicating ductile fracture were observed on the fracture surfaces in general of the samples, a cleavage fracture surface indicating brittle fracture was encountered in the tensile test specimen 3, which came out of the 10th production. It is considered that the reason for this may be a defect on the surface or a near-surface porosity for this specimen.

4.3.6 Heat Treatment of the Final Parts

In order to examine whether there is a change in the microstructure and hardness values of the parts obtained as a result of the production with reused powders

compared to the parts produced with unused powder, the heat treatment procedures were applied to the parts, the details of which are given in the subsection 3.5.7.

4.3.6.1 Cr_{eq}/Ni_{eq} Calculations

The microstructure of the part obtained in additive manufacturing depends on the chemical composition of the starting powders as mentioned in the literature review section. The Cr_{eq}/Ni_{eq} ratio appears as an indicator of whether the microstructure is ferritic or martensitic. So, first of all, Cr_{eq}/Ni_{eq} ratio was calculated.

Table 4.17 Cr_{eq}/Ni_{eq} calculations for 17-4 PH stainless steel used in production 1

Element	**Amount (wt%)**	**Cr_{eq}**	**Ni_{eq}**	**Cr_{eq}/Ni_{eq}**
Cr	16.76	16.95	6.42	2.64
Mo	0.00			
Nb	0.27			
Ni	4.23			
C	0.02			
N	0.03			
Cu	4.33			

Table 4.18 Cr_{eq}/Ni_{eq} calculations for 17-4 PH stainless steel used in production 10

Element	**Amount (wt%)**	**Cr_{eq}**	**Ni_{eq}**	**Cr_{eq}/Ni_{eq}**
Cr	16.65	16.85	6.75	2.49
Mo	0.00			
Nb	0.29			
Ni	4.39			
C	0.02			
N	0.03			
Cu	4.40			

The calculations in Table 4.17 and Table 4.18 were calculated according to the formula given in [18] where, Cr_{eq} = Cr + Mo + (0.7 x Nb) and Ni_{eq} = Ni + (35 x C) + (20 x N) + (0.25 x Cu). When Cr_{eq}/Ni_{eq} ratio is higher than 1.5, it is mentioned that the microstructure is obtained in delta ferritic structure [18]. When the results were examined, it was seen that Cr_{eq}/Ni_{eq} ratio decreased as the powders were reused but still remained in the ferritic range.

4.3.6.2 Microstructural Evaluation

The microstructures obtained before and as a result of the heat treatments for production 1 (P1) parts and production 10 (P10) parts are given in Figure 4.34 to Figure 4.38.

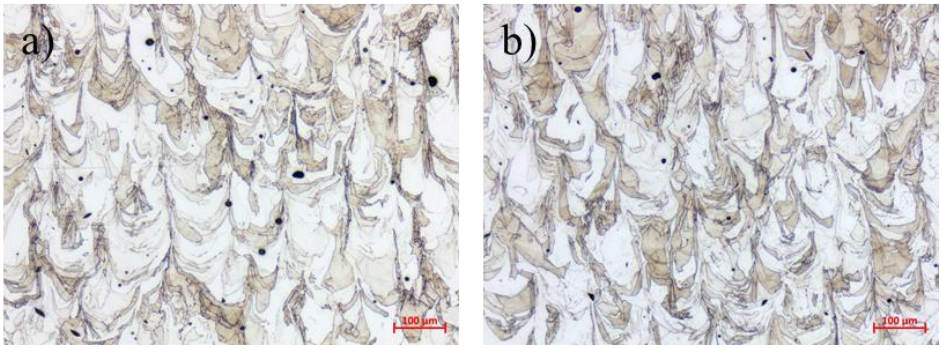

Figure 4.34. As-built microstructures of a) P1 and b) P10 (100x)

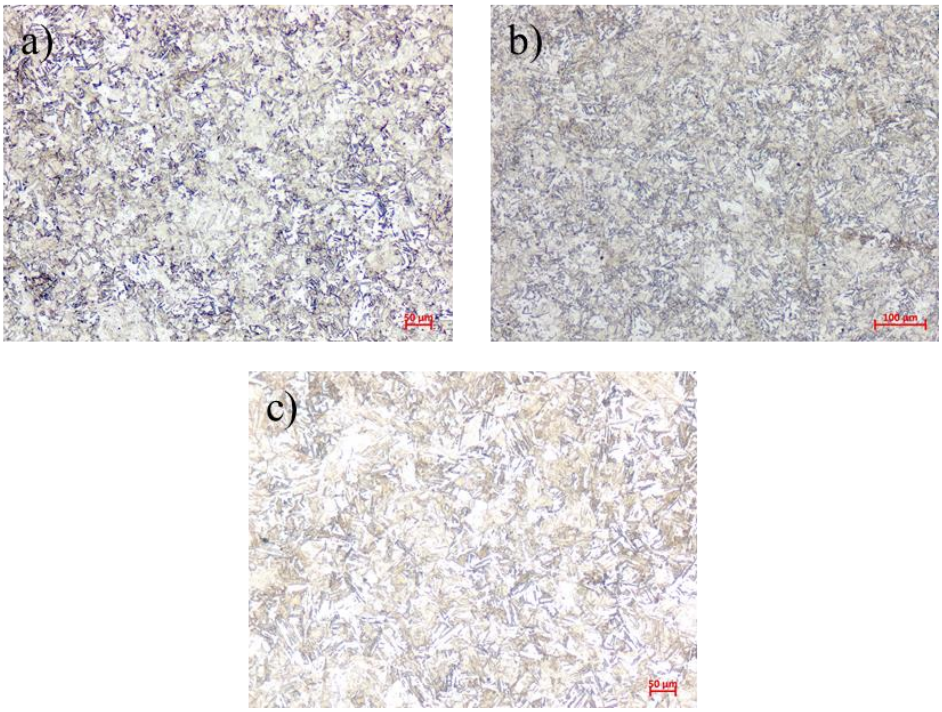

Figure 4.35. SHT microstructures of a) P1, b) P10 and c) conventional (100x)

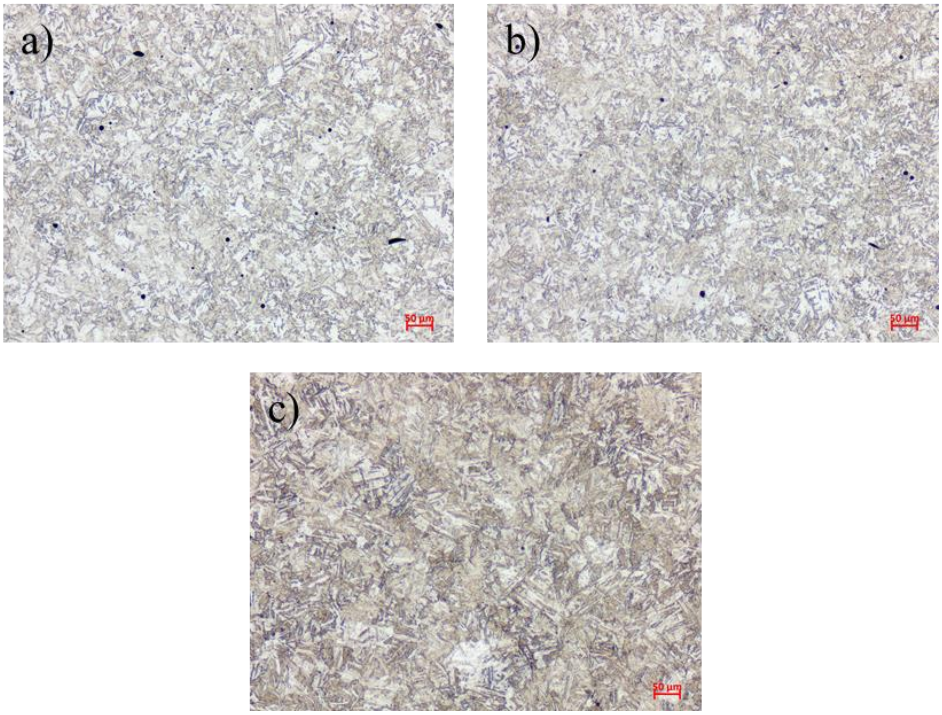

Figure 4.36. H900 microstructures of a) P1, b) P10 and c) conventional (100x)

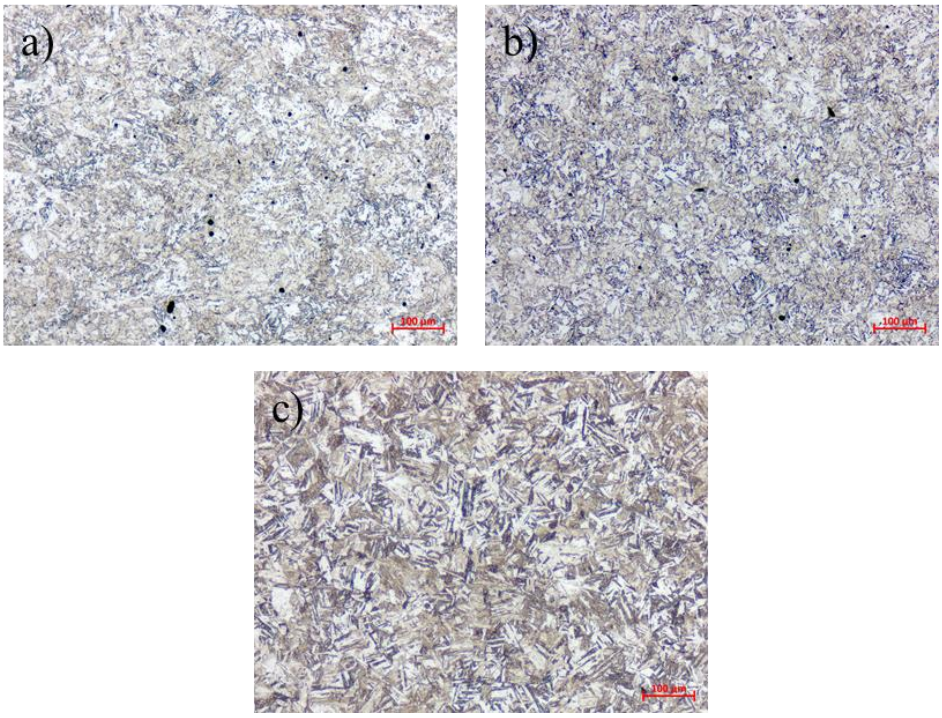

Figure 4.37. H1025 microstructures of a) P1, b) P10 and c) conventional (100x)

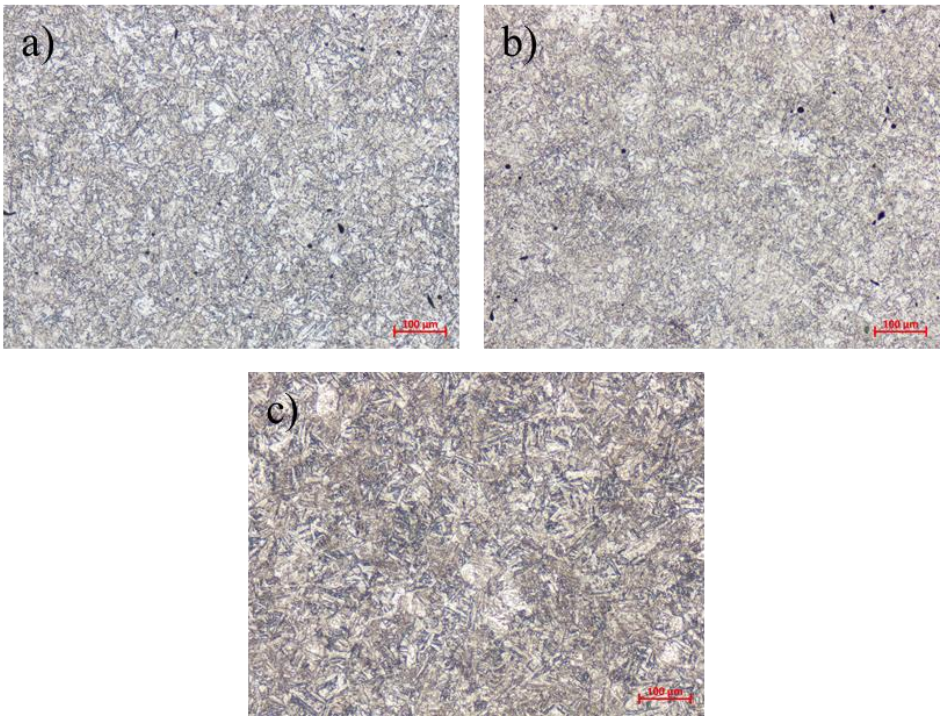

Figure 4.38. H1100 microstructures of a) P1, b) P10 and c) conventional (100x)

As-built microstructures obtained from both productions were columnar delta ferritic structure. When Cr_{eq}/Ni_{eq} ratios are examined, it is seen that results supporting this microstructure obtained. In all subsequent heat treatment conditions, martensitic microstructure was obtained in the parts. Grain sizes are similar to that of conventional material.

4.3.6.3 Hardness Measurements

Hardness measurements were carried out on the heat treatment coupons obtained by cutting the ends of the tensile test specimens obtained from 1st and 10th productions and produced from conventional material. The hardness values after heat treatments are given in Table 4.22 and are in agreement with the values given in ASTM A564M Standard Specification for Hot-Rolled and Cold-Finished Age-Hardening Stainless Steel Bars and Shapes [54].

Table 4.19 Hardness values for 17-4 PH SS after heat treatments (according to ASTM A564m)

Condition	*Hardness (HRC)*
SHT	Max. 38
H900	Min. 40
H1025	Min 35
H1100	Min. 31

The hardness values obtained from the as-built conditions and after being exposed to heat treatments can be seen in Table 4.20 to Table 4.22. When the results were examined, it was seen that the reuse of powder has no considerable effect on the as-built hardness of the material.

Table 4.20 Hardness results of production 1 (in HRC)

		As-Built	***SHT***	***H900***	***H1025***	***H1100***
Production 1	1	29.8	33.3	46.9	36.6	37.7
	2	32.2	33.3	40.8	38.8	35.5
	3	32.2	33.3	44.5	38.8	36.6
	4	32.2	32.2	45.3	38.8	36.6
	5	32.2	33.3	47.7	39.8	36.6
	Average	31.7	33.1	45.0	38.6	36.6
	St. Dev.	1.1	0.5	2.7	1.2	0.8
	Confidence Interval (95%)	1.3	0.6	3.3	1.5	1.0

Table 4.21 Hardness results of production 10 (in HRC)

		As-Built	***SHT***	***H900***	***H1025***	***H1100***
Production 10	1	31.0	34.4	46.9	36.6	35.5
	2	32.2	33.3	47.7	38.8	37.7
	3	33.3	32.2	47.7	37.7	35.5
	4	32.2	33.3	48.4	38.8	37.7
	5	32.2	33.3	48.4	36.6	37.7
	Average	32.2	33.3	47.8	37.7	36.8
	St. Dev.	0.8	0.8	0.6	1.1	1.2
	Confidence Interval (95%)	1.0	1.0	0.8	1.4	1.5

Table 4.22 Hardness results of conventional 17-4 PH SS (in HRC)

		SHT	***H900***	***H1025***	***H1100***
Conventional	1	37.7	43.6	36.6	35.5
	2	37.7	45.3	36.6	35.5
	3	36.6	45.3	37.7	35.5
	4	36.6	44.5	36.6	35.5
	5	36.6	45.3	36.6	34.4
	Average	37.0	44.8	36.8	35.3
	St. Dev.	0.6	0.8	0.5	0.5
	Confidence Interval (95%).	0.7	0.9	0.6	0.6

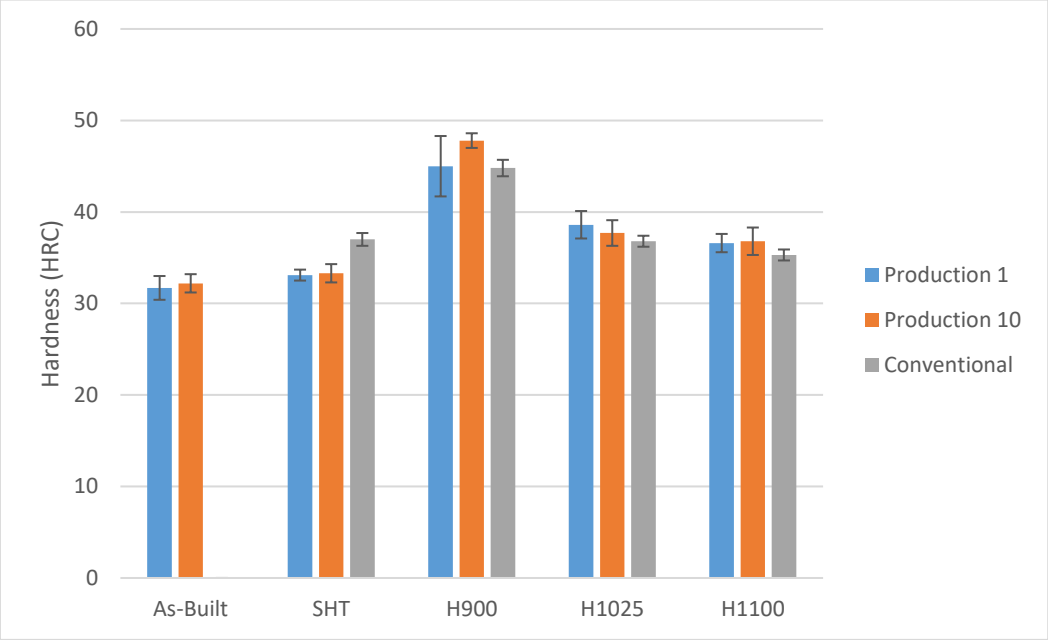

Figure 4.39. Hardness comparison chart

In all heat-treated cases, it has been observed that the parts meet the minimum values required in the standard. Although there is no difference between the parts in terms of hardness in the as-built condition, it is observed that there are changes in the hardness of the parts in the heat-treated condition. When SHT was made to the parts, it can be seen that the conventional material resulted in higher hardness than the additive manufacturing parts (conventional 17-4 PH SS: 37 HRC and AM 17-4 PH SS: 33 HRC). There is no significant difference between the 1^{st} and 10^{th} production. When the hardness of the parts in H900 condition is compared with SHT for 1 hour at 480°C, it was seen that the hardness values of the additive manufacturing parts reached to the hardness values of the conventional material. However, there was still no change in hardness with the reuse of the powder. The same result is valid for H1025 and H1100 conditions. As a result, there was no change in the hardness of the parts with 10 reuse of the powders. However, additive manufacturing parts whose hardness was less than the conventional 17-4 PH stainless steel when SHT is made, reached to that of the conventional material when they entered the aging heat treatment.

CHAPTER 5

CONCLUSION

In this thesis study, the effects of the reuse of 17-4 PH stainless steel powders in additive manufacturing using these powders were investigated. The results of this thesis work are listed below.

1. When the morphologies of the powders were examined under SEM, it is seen that the starting powders are slightly far from perfect sphericity. After 10 times use, powders with slightly more distorted shape is seen when compared to that of the unused powder sample.
2. The bulk density value decreased by 3.2%, however, the tapped density value remained the same with powder reuse. The flow rate of powders decreased with reuse. The density measured from the first production to the last production decreased by 0.3%, it can be concluded that there is no significant change in the Archimedes density value. Optical occupancy analysis results performed with the ImageJ program also showed a small decrease in occupancy with the reuse of powders.
3. While the chemical composition of the powders did not change on the basis of main elements, it was observed that the oxygen and nitrogen content of the powders are increased. After reuse of 10 times, the amount of oxygen in the powder increased by 16% and the amount of nitrogen increased by 17% which is most probably due to contact of the powders with air during handling. When EDS analysis was performed on the chemical composition of the parts, it was observed that the copper content of the produced parts gradually decreased as the powders were reused.
4. Reusing the powders 10 times does not cause a detrimental effect on the tensile properties of the material produced from these powders.

5. It has been observed that the microstructure of the specimens after additive manufacturing consists of delta ferrite. Even if the Cr_{eq}/Ni_{eq} ratio decreased by repetitive use of the powders, the composition remained in the delta ferrite region. When SHT was applied, the delta ferrite structure was completely eliminated in both the 1st production parts and the 10th production parts, and a martensitic microstructure was obtained.
6. In the case of SHT, the conventional 17-4 PH stainless steel had a higher hardness value than when produced by additive manufacturing. However, after aging heat treatments to reach H900, H1025 and H1100 conditions, the hardness value of additively manufactured 17-4 PH stainless steel reached the hardness value of conventional material. With the reuse of the powder, no change was found in the hardnesses as a result of heat treatment.

REFERENCES

[1] Rafi, H. K., Pal, D., Patil, N., Starr, T. L., & Stucker, B. E. (2014). Microstructure and Mechanical Behavior of 17-4 Precipitation Hardenable Steel Processed by Selective Laser Melting. Journal of Materials Engineering and Performance, 23(12), 4421–4428. https://doi.org/10.1007/s11665-014-1226

[2] ASTM F2792-12a. (2013). Standard Terminology for Additive Manufacturing Technologies. ASTM International. pp. 1-3. West Conshohocken, PA.

[3] ASTM F2924-14. (2014). Standard Specification for Additive Manufacturing Titanium-6 Aluminum-4 Vanadium with Powder Bed Fusion. ASTM International. West Conshohocken, PA.

[4] ASTM F3055-14a. (2014). Standard Specification for Additive Manufacturing Nickel Alloy (UNS N07718) with Powder Bed Fusion. ASTM International. West Conshohocken, PA.

[5] Cordova, L., Campos, M. & Tinga, T. (2019). Revealing the Effects of Powder Reuse for Selective Laser Melting by Powder Characterization. JOM, 71(3), 1062-1072. https://doi.org/10.1007/s11837-018-3305-2

[6] Calignano, F., Manfredi, D., Ambrosio, E. P., Biamino, S., Lombardi, M., Atzeni, E., Salmi, A., Minetola, P., Iuliano, L., & Fino, P. (2017). Overview on Additive Manufacturing Technologies. Proceedings of the IEEE, 105(4), 593–612. https://doi.org/10.1109/jproc.2016.2625098

[7] Stampfl, J., & Hatzenbichler, M. (2014). Additive Manufacturing Technologies. CIRP Encyclopedia of Production Engineering, 20–27. https://doi.org/10.1007/978-3-642-20617-7_6492

[8] Attaran, M. (2017). The rise of 3-D printing: The advantages of additive manufacturing over traditional manufacturing. Business Horizons, 60(5), 677–688. https://doi.org/10.1016/j.bushor.2017.05.011

[9] Schleifenbaum, H., Diatlov, A., Hinke, C., Bültmann, J., & Voswinckel, H. (2011). Direct photonic production: towards high speed additive manufacturing of individualized goods. Production Engineering, 5(4), 359–371. https://doi.org/10.1007/s11740-011-0331-0

[10] Kruth, J.-P., Levy, G., Klocke, F., & Childs, T. H. C. (2007). Consolidation phenomena in laser and powder-bed based layered manufacturing. CIRP Annals, 56(2), 730–759. https://doi.org/10.1016/j.cirp.2007.10.004

[11] Kruth, J.-P., Badrossamay, M., Yasa, E., Deckers, J., Thijs, L. and Humbeeck, J. V. (2010). Part and material properties in selective laser melting of metals. 16th International Symposium on Electromachining (ISEM XVI).

[12] Bremen, S., Meiners, W., & Diatlov, A. (2012). Selective Laser Melting. Laser Technik Journal, 9(2), 33–38. https://doi.org/10.1002/latj.201290018

[13] Yap, C. Y., Chua, C. K., Dong, Z. L., Liu, Z. H., Zhang, D. Q., Loh, L. E., & Sing, S. L. (2015). Review of selective laser melting: Materials and applications. In Applied Physics Reviews (Vol. 2, Issue 4). American Institute of Physics Inc. https://doi.org/10.1063/1.4935926

[14] Zai, L., Zhang, C., Wang, Y., Guo, W., Wellmann, D., Tong, X., & Tian, Y. (2020). Laser powder bed fusion of precipitation-hardened martensitic stainless steels: A review. In Metals (Vol. 10, Issue 2). MDPI AG. https://doi.org/10.3390/met10020255

[15] Dutta, S. K. (n.d.). Different Types and New Applications of Stainless Steel Processing of Low-grade Iron Ore View project Development of new alloys View project Different Types and New Applications of Stainless Steel. https://www.researchgate.net/publication/330383386

[16] Wing, J., Zou2', H., Li, C., Zuo3', R., Qiu'', S., & Shen, B. (2006). Materials Relationship of microstructure transformation and hardening behavior of type 17-4 PH stainless steel. In Journal of University of Science and Technology Beijing (Vol. 13, Issue 3).

[17] Haghdadi, N., Laleh, M., Moyle, M., & Primig, S. (2021). Additive manufacturing of steels: a review of achievements and challenges. In Journal of

Materials Science (Vol. 56, Issue 1, pp. 64–107). Springer. https://doi.org/10.1007/s10853-020-05109-0

[18] Sabooni, S., Chabok, A., Feng, S. C., Blaauw, H., Pijper, T. C., Yang, H. J. & Pei, Y. T. (2021). Laser powder bed fusion of 17–4 PH stainless steel: A comparative study on the effect of heat treatment on the microstructure evolution and mechanical properties. Additive Manufacturing, 46. https://doi.org/10.1016/j.addma.2021.102176

[19] Alnajjar, M., Christien, F., Bosch, C. & Wolski, K. (2020). A comparative study of microstructure and hydrogen embrittlement of selective laser melted and wrought 17–4 PH stainless steel. Materials Science & Engineering A. 785. https://doi.org/10.1016/j.msea.2020.139363

[20] Ozsoy, A., Yasa, E., Keles, M., & Tureyen, E. B. (2021). Pulsed-mode Selective Laser Melting of 17-4 PH stainless steel: Effect of laser parameters on density and mechanical properties. Journal of Manufacturing Processes, 68, 910–922. https://doi.org/10.1016/j.jmapro.2021.06.017

[21] Dietrich, S., Wunderer, M., Huissel, A., & Zaeh, M. F. (2016). A New Approach for a Flexible Powder Production for Additive Manufacturing. Procedia Manufacturing, 6, 88–95. https://doi.org/10.1016/j.promfg.2016.11.012

[22] Slotwinski, J. A., Garboczi, E. J., Stutzman, P. E., Ferraris, C. F., Watson, S. S., & Peltz, M. A. (2014). Characterization of metal powders used for additive manufacturing. Journal of Research of the National Institute of Standards and Technology, 119, 460–493. https://doi.org/10.6028/jres.119.018

[23] Pleass, C., & Jothi, S. (2018). Influence of powder characteristics and additive manufacturing process parameters on the microstructure and mechanical behaviour of Inconel 625 fabricated by Selective Laser Melting. Additive Manufacturing, 24, 419–431. https://doi.org/10.1016/j.addma.2018.09.023

[24] Lutter-Günther, M., Bröker, M., Mayer, T., Lizak, S., Seidel, C., & Reinhart, G. (2018). Spatter formation during laser beam melting of AlSi10Mg and effects on powder quality. Procedia CIRP, 74, 33–38. https://doi.org/10.1016/j.procir.2018.08.008

[25] Asgari, H., Baxter, C., Hosseinkhani, K., Mohammadi, M. (2017). On microstructure and mechanical properties of additively manufactured AlSi10Mg_200C using recycled powder. Mater. Sci. Eng. A 707, 148–158.

[26] Jelis, E., Clemente, M., Kerwien, S., Ravindra, N.M., Hespos, M.R. (2015). Metallurgical and mechanical evaluation of 4340 steel produced by direct metal laser sintering. JOM.

[27] Maamoun, A.H., Elbestawi, M., Dosbaeva, G.K., Veldhuis, S.C., 2018. Thermal post processing of AlSi10Mg parts produced by Selective Laser Melting using recycled powder. Addit. Manuf. 21, 234–247.

[28] Gruber, H., Karimi, P., Hryha, E., Nyborg, L., 2018. Effect of powder recycling on the fracture behavior of Electron beam melted alloy 718. Powder Metall.

[29] Spierings, A.B., Herres, N., Levy, G., 2011. Influence of the particle size distribution on surface quality and mechanical properties in AM steel parts. Rapid Prototyp. J. 17, 195–202.

[30] Delgado, J., Ciurana, J., Rodríguez, C.A., 2012. Influence of process parameters on part quality and mechanical properties for DMLS and SLM with iron-based materials. Int. J. Adv. Manuf. Technol.

[31] Terrassa, K.L., Haley, J.C., MacDonald, B.E., Schoenung, J.M., 2018. Reuse of powder feedstock for directed energy deposition. Powder Technol. 338, 819–829.

[32] Tang, H.P., Qian, M., Liu, N., Zhang, X.Z., Yang, G.Y., Wang, J., 2015. Effect of powder reuse times on additive manufacturing of Ti-6Al-4V by selective Electron beam melting. JOM.

[33] Smith, W.F. (1981). Structure and Properties of Engineering Alloys. McGraw-Hill Book. New York, NY.

[34] Lin, X., Cao, Y., Wu, X., Yang, H., Chen, J. and Huang, W. (2012). Microstructure and mechanical properties of laser forming repaired 17-4PH stainless steel. Materials Science and Engineering. 553. 80-88.

[35] Hsiao, C.N., Chiou, C.S., Yang, J.R., 2002. Aging reactions in a 17-4 PH stainless steel. Mater. Chem. Phys.

[36] Zapico, P., Giganto, S., Barreiro, J. and Martinez-Pellitero, S. (2020). Characterisation of 17-4 PH Metallic Powder Recycling to Optimise the Performance of the Selective Laser Melting Process. JMR&T. 9(2). 1273-1285.

[37] Ahmed, F., Ali, U, Sarker, D, Marzbanrad, E. and Choi, K. (2019). Study of powder recycling and its effect on printed parts during laser powder-bed fusion of 17-4 PH stainless steel. Journal of Materials Processing Tech. 278.

[38] Aboulkhair, N.T., Everitt, N.M., Ashcroft, I., Tuck, C., 2014. Reducing porosity in AlSi10Mg parts processed by selective laser melting. Addit. Manuf. 1, 77–86.

[39] Gu D, Xia M, Dai D. On the role of powder flow behavior influid thermodynamics and laser processability of Ni-basedcomposites by selective laser melting. Int J Mach ToolsManuf 2019;137:67– 78.

[40] Murr LE, Martínez E, Hernández J, Collins S, Amato KN,Gaytan SM, et al. Microstructures and properties of 17-4PHstainless steel fabricated by selective laser melting. J MaterRes Technol 2012;1(3):167–77.

[41] Yablokova G, Speirs M, Van Humbeeck J, Kruth JP, Schrooten J,Cloots R, et al. Rheological behavior of Ti and NiTi powdersproduced by atomization for SLM production of open porousorthopedic implants. Powder Technol 2015;283:199–209.

[42] ASTM E8m-04. (2004). Standard Test Methods for Tension Testing of Metallic Materials [Metric]. ASTM International. West Conshohocken, PA.

[43] ASTM B215-04. (2004). Standard Practices for Sampling Metal Powders. ASTM International. West Conshohocken, PA.

[44] ASTM E1019-11. (2011). Standard Test Methods for Determination of Carbon, Sulfur, Nitrogen, and Oxygen in Steel and in Iron, Nickel, and Cobalt Alloys. ASTM International. West Conshohocken, PA.

[45] ASTM E1941-04. (2004). Standard Test Method for Determination of Carbon in Refractory and Reactive Metals and Their Alloys. ASTM International. West Conshohocken, PA.

[46] ASTM E1479-99. (1999). Standard Practice for Describing and Specifying Inductively-Coupled Plasma Atomic Emission Spectrometers. ASTM International. West Conshohocken, PA.

[47] ASTM B212-99. (1999). Standard Test Method for Apparent Density of Free-Flowing Metal Powders Using the Hall Flowmeter Funnel. ASTM International. West Conshohocken, PA.

[48] ASTM B527-93. (1993). Standard Test Method for Determination of Tap Density of Metallic Powders and Compounds. ASTM International. West Conshohocken, PA.

[49] ASTM B213-03. (2003). Standard Test Method for Flow Rate of Metal Powders. ASTM International. West Conshohocken, PA.

[50] Powell, D., Rennie, A. E. W., Geekie, L., & Burns, N. (2020). Understanding powder degradation in metal additive manufacturing to allow the upcycling of recycled powders. In Journal of Cleaner Production (Vol. 268). Elsevier Ltd. https://doi.org/10.1016/j.jclepro.2020.122077

[51] Sun, Y., Aindow, M., & Hebert, R. J. (2018). Comparison of virgin Ti-6Al-4V powders for additive manufacturing. Additive Manufacturing, 21, 544–555. https://doi.org/10.1016/j.addma.2018.02.011

[52] Dobson, S., Vunnam, S., Frankel, D., Sudbrack, C., & Starr, T. (n.d.). Powder Variation And Mechanical Properties For Slm 17-4 Ph Stainless Steel.

[53] Conesa, C., Saleh, K., Thomas, A., Guigon, P. & Guillot, N. (2004). Characterization of Flow Properties of Powder Coatings Used in the Automotive Industry. Kona. No.22. 94-106.

[54] ASTM A564-10. (2010). Standard Specification for Hot-Rolled and Cold-Finished Age-Hardening Stainless Steel Bars and Shapes. ASTM International. West Conshohocken, PA.